



Published in final edited form as:

Immunity. 2019 July 16; 51(1): 50–63.e5. doi:10.1016/j.immuni.2019.05.005.

Inflammasome Regulates Hematopoiesis through Cleavage of the Master Erythroid Transcription Factor GATA1

Sylwia D. Tyrkalska^{1,10,12}, Ana B. Pérez-Oliva^{1,12,*}, Lola Rodríguez-Ruiz¹, Francisco J. Martínez-Morcillo¹, Francisca Alcaraz-Pérez², Francisco J. Martínez-Navarro¹, Christophe Lachaud³, Nouraiz Ahmed⁴, Timm Schroeder⁴, Irene Pardo-Sánchez¹, Sergio Candel^{1,11}, Azucena López-Muñoz¹, Avik Choudhuri^{5,6}, Marlies P. Rossmann^{5,6}, Leonard I. Zon^{5,6,7,8,9}, María L. Cayuela², Diana García-Moreno^{1,*}, Victoriano Mulero^{1,13,*}

¹Departamento de Biología Celular e Histología, Facultad de Biología, Universidad de Murcia, IMIB-Arixaca, Murcia, Spain ²Hospital Clínico Universitario Virgen de la Arrixaca, IMIB-Arixaca, Murcia, Spain ³Aix-Marseille University, Inserm, CNRS, Institut Paoli-Calmettes, CRCM, Marseille, France ⁴Department of Biosystems Science and Engineering, ETH Zurich, Basel, Switzerland ⁵Department of Stem Cell and Regenerative Biology, Harvard University, Cambridge, MA 02138, USA ⁶Stem Cell Program and Division of Hematology/Oncology, Children's Hospital Boston, Howard Hughes Medical Institute, Boston, MA 02115, USA ⁷Dana-Farber Cancer Institute, Boston, MA 02215, USA ⁸Harvard Stem Cell Institute, Boston, MA 02115, USA ⁹Harvard Medical School, Boston, MA 02115, USA ¹⁰Present address: Cambridge Institute for Medical Research, University of Cambridge, Cambridge CB2 0XY, UK ¹¹Present address: Department of Medicine, University of Cambridge, MRC Laboratory of Molecular Biology, Cambridge CB2 0QH, UK ¹²These authors contributed equally ¹³Lead contact

SUMMARY

Chronic inflammatory diseases are associated with altered hematopoiesis that could result in neutrophilia and anemia. Here we report that genetic or chemical manipulation of different inflammasome components altered the differentiation of hematopoietic stem and progenitor cells (HSPC) in zebrafish. Although the inflammasome was dispensable for the emergence of HSPC, it was intrinsically required for their myeloid differentiation. In addition, Gata1 transcript and protein amounts increased in inflammasome-deficient larvae, enforcing erythropoiesis and inhibiting myelopoiesis. This mechanism is evolutionarily conserved, since pharmacological inhibition of the inflammasome altered erythroid differentiation of human erythroleukemic K562 cells. In addition, caspase-1 inhibition rapidly upregulated GATA1 protein in mouse HSPC promoting their erythroid differentiation. Importantly, pharmacological inhibition of the inflammasome rescued zebrafish disease models of neutrophilic inflammation and anemia. These

*Correspondence: anabpo@um.es (A.B.P.-O.), dianagm@um.es (D.G.-M.), vmulero@um.es (V.M.).

AUTHOR CONTRIBUTIONS

V.M. conceived the study; S.D.T., A.B.P.-O., C.L., T.S., L.I.Z., M.L.C., D.G.-M., and V.M. designed research; S.D.T., A.B.P.-O., L.R.-R., F.J.M.-M., F.A.-P., F.J.M.-N., C.L., N.A., I.P.-S., S.C., A.L.-M., A.C., M.P.R., and D.G.-M. performed research; S.D.T., A.B.P.-O., L.R.-R., F.J.M.-M., F.A.-P., F.J.M.-N., C.L., N.A., T.S., I.P.-S., S.C., A.L.-M., A.C., M.P.R., L.I.Z., M.L.C., D.G.-M., and V.M. analyzed data; and S.D.T. and V.M. wrote the manuscript with minor contribution from other authors.

SUPPLEMENTAL INFORMATION

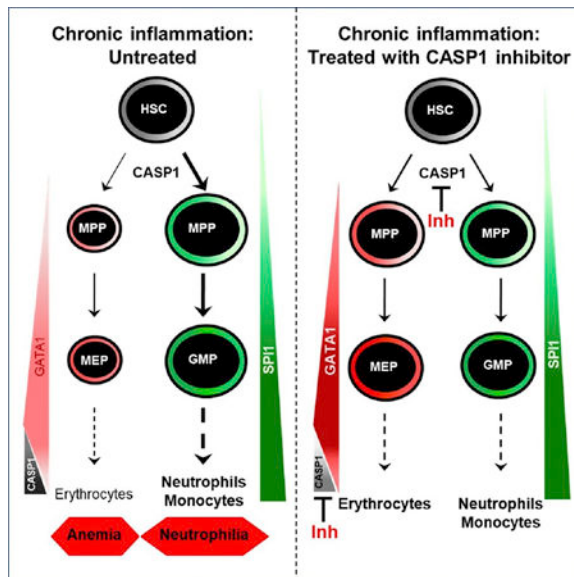
Supplemental Information can be found online at <https://doi.org/10.1016/j.immuni.2019.05.005>.

results indicate that the inflammasome plays a major role in the pathogenesis of neutrophilia and anemia of chronic diseases and reveal druggable targets for therapeutic interventions.

In Brief

Chronic inflammatory diseases are associated to altered hematopoiesis that could result in neutrophilia and anemia. In this issue of *Immunity*, Tyrkalska et al. (2019) provide evidence of an evolutionary conserved mechanism by which inflammasome regulates the erythroid/myeloid decision in HSC, which might contribute to the hematopoietic bias of these diseases.

Graphical Abstract



INTRODUCTION

Hematopoiesis is the process of blood cell formation that occurs during embryonic development and across adulthood to produce the blood system (Jagannathan-Bogdan and Zon, 2013). In vertebrates, blood development involves two main waves of hematopoiesis: the primitive one during early embryonic development and the definitive one, which occurs in later stages (Gore et al., 2018). Definitive hematopoiesis engages multipotent hematopoietic stem cells (HSCs), which migrate eventually to the bone marrow, or kidney marrow in zebrafish, and give rise to all blood lineages (Birbrair and Frenette, 2016; Cumano and Godin, 2007). HSC maturation involves the diversification of the lymphoid (T, B, and NK cells) and myeloid and erythroid cell lineages (megakaryocytes, erythrocytes, granulocytes, and macrophages) (Kondo, 2010; Kondo et al., 2003; Weissman, 2000). The decision for erythroid and myeloid fates depends mainly on two transcription factors, GATA1 and SPI1 (also known as PU.1), that show a cross-inhibitory relationship resulting in physical interaction and direct competition between them for target genes (Nerlov et al., 2000; Rekhtman et al., 1999). However, there are many controversies about the factors responsible for terminal erythroid and myeloid differentiation and many unknown pathways

probably being involved in its regulation (Cantor and Orkin, 2002; Hoppe et al., 2016). These unidentified pathways might have important clinical implications, because hematopoietic lineage bias is associated with increased incidence of diseases with prominent inflammatory components including atherosclerosis, autoimmunity, neurodegenerative disease, and carcinogenesis (Elias et al., 2017).

The inflammasomes are part of innate immune system and as intracellular receptors and sensors, they regulate the activation of inflammatory caspases, namely caspase-1 and caspase-11, which induce inflammation in response to infectious microbes and endogenous danger signals (Latz et al., 2013; Martinon et al., 2009). Typically inflammasome multiprotein complexes contain sensor proteins (nucleotide binding domain and leucine rich repeat gene family, NLRs), adaptor proteins (apoptosis-associated speck-like protein containing a CARD, ASC), and effector caspases in a zymogen form, all being able to interact among themselves by homotypic interactions (Broz and Monack, 2011; Sharma and Kanneganti, 2016). Recently, it has been shown that also guanylate binding protein (GBP) protein family forms part of these multiprotein complexes (Pilla et al., 2014; Santos et al., 2018; Tyrkalska et al., 2016; Wallet et al., 2017; Zwack et al., 2017). Oligomerization of pro-caspases and their autoproteolytic maturation lead to the processing and secretion of the pro-inflammatory cytokines interleukin-1 β (IL-1 β) and IL-18, and the induction of a form of programmed cell death called pyroptosis (Lamkanfi and Dixit, 2014). Lately, it has been reported that inflammasomes play crucial roles not only in infection and sterile inflammation but also in maintaining the basic cellular functions and controlling cellular homeostasis (Rathinam and Fitzgerald, 2016). Hence, additional uncovered regulatory functions for the inflammasomes have been shown in cell metabolism, proliferation, gene transcription and tumorigenesis (Rathinam and Fitzgerald, 2016; Sharma and Kanneganti, 2016). Although up to date little is known about the impact of the inflammasomes on hematopoiesis in general, it has been shown that the master erythroid transcription factor GATA1 can be cleaved *in vitro* by many caspases and *in vivo* by caspase-3 (De Maria et al., 1999).

Zebrafish has recently arisen as a powerful and useful model to study hematopoiesis (Berman et al., 2012; Ellett and Lieschke, 2010). Moreover, the genetic programs controlling hematopoiesis in the zebrafish are conserved with mammals, including humans, making them clinically relevant model systems (Jagannathan-Bogdan and Zon, 2013). Here we show the critical role played by the inflammasome in the regulation of erythroid and myeloid cell-fate decision, and terminal erythroid differentiation. Furthermore, the results also have important clinical implications, since pharmacological inhibition of the inflammasome rescued zebra-fish disease models of neutrophilic inflammation and anemia.

RESULTS

Inflammasome Inhibition Decreases the Number of Neutrophils and Macrophages in Zebrafish Larvae

Using zebrafish transgenic lines with green fluorescent neutrophils *Tg(mpx:eGFP)ⁱ¹¹⁴* or macrophages *Tg(mpeg1:eGFP)^{g122}*, we quantitated the total number of both cell populations in whole larvae at 72 hpf. Genetic inhibition of several inflammasome components, namely

Gbp4 and Asc resulted in significant decreased numbers of both neutrophils (Figures 1A and 1B) and macrophages (Figures S1A and S1B). Similarly, pharmacological inhibition of caspase-1 with the irreversible inhibitor Ac-YVAD-CMK (Tyrkalska et al., 2016) also resulted in decreased numbers of myeloid cells (Figures 1C, 1D, S1C, S1D). These results were confirmed using an independent transgenic line *Tg(lyz:dsRED)^{mz50}* with labeled neutrophils (Figures S2A–S2D). Similarly, forced expression of the GTPase-deficient mutant of Gbp4 (KS/AA) as well as its double mutant (DM: KS/AA; CARD), both of which behave as dominant negatives (DN) and inhibit inflammasome-dependent caspase-1 activation (Tyrkalska et al., 2016), resulted in decreased neutrophil number (Figures 1E and 1F). In addition, although activation of the inflammasome by forced expression of either Gbp4 or Asc failed to increase neutrophil (Figures 1E–1H) or macrophage (Figures S1E and S1F) numbers, it was able to rescue myeloid cell number and caspase-1 activity in Asc-deficient fish (Figures 1G and 1H). Notably, however, simultaneous expression of Asc and Caspa, the functional homolog of mammalian CASP1 (Kuri et al., 2017; Masumoto et al., 2003; Tyrkalska et al., 2016), significantly increased the number of neutrophils (Figures 1I and 1J) and macrophages (Figures S1E and S1F).

The Inflammasome Regulates HSPC Differentiation but Is Dispensable for Their Emergence

The differentiation of hematopoietic stem and progenitor cells (HSPC) into various blood cell types is controlled by multiple extrinsic and intrinsic factors and the deregulation in hematopoiesis can result in a number of hematological abnormalities (Morrison et al., 1997; Yang et al., 2007). Chronic inflammatory disorders are usually associated to neutrophilia and anemia, the so-called anemia of chronic diseases (ACD). Therefore, we next examined whether the inflammasome also regulated erythropoiesis using a zebrafish transgenic line *Tg(lcr:eGFP)*, which has specific erythroid GFP expression (Ganis et al., 2012). The results showed that inflammasome activity had the inverse effect on erythrocytes than on myeloid cells; that is, erythrocyte abundance increased following genetic and pharmacological inflammasome inhibition, as assayed by flow cytometry (Figures 1K and 1L and S3). However, the expression of *cmyb* and *runx1*, which begins by 36hpf and marks emerging definitive HSPC (Burns et al., 2005), was unaffected in guanylate binding protein-4 (Gbp4)- and Asc-deficient larvae at 48 hpf, as assayed by whole-mount *in situ* hybridization (WISH) (Figure S4). Similarly, the expression of *rag1*, which is expressed in differentiated thymic T cells, was apparently unaffected by 5 dpf in inflammasome-deficient larvae (Figure S4). Collectively, these results suggest a specific role of the inflammasome in the regulation of the balance between myelopoiesis and erythropoiesis.

To further confirm the role of the inflammasome in HSPC differentiation, we quantitated the number of HSPC in the transgenic line *Tg(runx1:GAL4; UAS:nfsB-mCherry)*, which has fluorescently labeled HSPC (Tamplin et al., 2015), upon genetic or pharmacological inhibition of the inflammasome at different developmental stages (24 and 48 hpf). Inhibition of caspase-1 resulted in no changes in HSPC number at any point of the treatment, the result being confirmed in Asc-deficient larvae (Figures 2A–2H). Furthermore, genetic inhibition of the inflammasome in neutrophils and HSPC by forced expression of DN forms of Asc (Asc CARD) or Gbp4 (Gbp4KS/AA) (Tyrkalska et al., 2016) using the specific promoters

mpx and *runx1*, respectively, showed that the number of neutrophils declined in HSPC, but not in neutrophil, inflammasome-deficient larvae (Figures 2I–2L). Collectively, these results confirm the dispensability of the inflammasome for HSPC emergence and renewal, but that is intrinsically required for HSPC differentiation.

Zebrafish is an elegant model for cell ablation by use of the specific transgenic lines that expresses the bacterial nitroreductase, encoded by the *nfsB* gene, under the control of specific promoters (Davison et al., 2007). The nitroreductase enzyme converts the drug metronidazole (Mtz) to a cytotoxic product, which induces cell death in expressing cells to achieve tissue-specific ablation having no effect on other cell populations (Curado et al., 2007, 2008; Prajsnar et al., 2012). Using this approach, we ablated neutrophils in *Tg(mpx:Gal4; UASnfsB-mCherry)* zebrafish by applying Mtz for 24 h and then analyzed neutrophil recovery in the presence or absence of the cas-pase-1 inhibitor for 6 days (Figure 3). Mtz robustly reduced neutrophil numbers, which began to recover by 4 days postablation in control larvae (Figure 3). However, pharmacological inhibition of the inflammasome impaired neutrophil recovery upon ablation and strongly decreased neutrophil abundance in non-ablated larvae (Figure 3). As expected, continuous Mtz treatment resulted in drastic neutrophil decline but did not show any toxic effect on control larvae that did not express the nitroreductase (Figure 3). These results indicate that the inflammasome is indispensable for myeloid differentiation of HSPC.

Inflammasome Inhibition Impairs Demand-Driven Myelopoiesis

In response to infection, the hematopoietic tissue enhances production and mobilization of neutrophils, which have short lifespan and are needed in large numbers to fight infections. This process is called demand-driven or emergency hematopoiesis (Hall et al., 2012). To check whether only steady-state or also demand-driven hematopoiesis were regulated by the inflammasome, we infected 48 hpf larvae with *Salmonella enterica* serovar Typhimurium in the otic vesicle and counted total neutrophil numbers at 24 hpi in the presence or absence of the irreversible caspase-1 inhibitor Ac-YVAD-CMK. It was observed that pharmacological inhibition of the inflammasome was able to abrogate infection-driven myelopoiesis, which resulted in increased number of neutrophils in infected larvae (Figures 4A and 4B). Notably, forced expression of granulocyte colony-stimulating factor (Gcsf), which stimulates both steady-state and demand-driven granulopoiesis in zebrafish (Hall et al., 2012; Stachura et al., 2013), increased neutrophil number to similar amounts in wild-type and Asc-deficient larvae, as well as in larvae treated with the caspase-1 inhibitor, without affecting cas-pase-1 activity (Figures 4C–4F). Nevertheless, Gcsf was unable to rescue the higher susceptibility to *S. Typhimurium* infection of Asc-deficient and caspase-1 inhibitor-treated larvae (Figures 4G and 4H), confirming previous results in Gbp4-deficient larvae (Tyrkalska et al., 2016). All these results also suggest that the inflammasome regulates the myeloid and erythroid fate decision besides the function of mature myeloid cells.

The Inflammasome Shifts the Spi1/Gata1 Balance Favoring Myeloid Differentiation

The regulation of Spi1 and Gata1 has been shown to be critical for the differentiation of myeloid and erythroid cells, respectively, in all vertebrates. As inhibition of the inflammasome resulted in a hematopoietic lineage bias, that is, reduced myeloid and

increased erythroid blood cells, we next analyzed *spi1* and *gata1* transcript amounts by RT-qPCR and whole-mount *in situ* hybridization (WISH). We observed decreased *spi1/gata1* transcript ratio at 24 hpf in Gbp4- and Asc-deficient larvae, while the transcript amounts of the genes encoding Spi1-downstream pivotal macrophage and neutrophil growth factors, namely macrophage and granulocyte colony-stimulating factors (*mcsf* and *gcsf* genes), were unaffected (Figures 4I and S4). Importantly, Gata1 protein amounts were also fine-tuned by the inflammasome, because genetic inhibition of either Asc or Gbp4 was able to increase Gata1, while forced expression of Asc and Caspa, which resulted in increased number of neutrophils and macrophages (Figure 1I, 1J, S1E, S1F), robustly decreased Gata1 (Figure 4J). Therefore, the inflammasome regulates HSPC fate decision through fine-tuning Gata1 amounts.

The Regulation of HSPC Differentiation by the Inflammasome Is Evolutionarily Conserved

We next sought to determine whether the inflammasome also regulates mouse hematopoiesis. We quantified the impact of CASP1 inhibition on GATA1 and SPI1 protein amounts in single mouse hematopoietic stem cells (HSC) using time-lapse microscopy immediately following their isolation. Time-lapse movies were acquired for 24 h to quantify early dynamics in GATA1 amounts before the first cell division using a homozygous and extensively validated GATA1 and SPI1 reporter mouse line expressing a fusion of GATA1 and monomeric Cherry (mCherry) and SPI1 and enhanced yellow fluorescent protein (eYFP) from the endogenous *Gata1* and *Spi1* genomic loci, respectively (Hoppe et al., 2016). Inhibition of CASP1 upregulated GATA1-mCherry protein in differentiating HSC within 18 h, while SPI1-eYFP protein amounts were unaffected (Figures 5A–5C). In line with these results, CASP1 inhibition increased megakaryocyte-erythrocyte (MegE) colony output of mouse HSCs at expense of granulocyte-monocyte (GM) colonies (Figure 5D). These data demonstrate that at the time of normal lineage decision making in HSC, the manipulation of GATA1 protein amounts through the inflammasome can alter lineage choice, further confirming our *in vivo* studies in zebrafish.

To further explore the relevance of the inflammasome in erythroid differentiation, we then used the human erythroleukemia K562 cell line, which can be differentiated to erythrocytes in the presence of hemin (Andersson et al., 1979; Koeffler and Golde, 1980). GATA1 amounts and activity were found to increase in the early stages of erythropoiesis, while they decreased in the late phase to allow terminal erythroid differentiation (Ferreira et al., 2005; Whyatt et al., 2000). As expected, we observed that hemin promoted gradual hemoglobin accumulation and decreased GATA1 protein amounts from 0 to 48 h (Figures 6A and 6D). Notably, the transcript amounts of *NLRC4*, *NLRP3*, and *CASP1* gradually increased, while those of *PYCARD* peaked at 12 h and then declined to basal amounts (Figure S5). Furthermore, CASP1 activity (Figure 6B) and protein amounts (Figure 6C) progressively increased during erythroid differentiation, and CASP1 was uniformly distributed in both the cytosol and the nucleus (Figure 6C). In addition, pharmacological inhibition of CASP1 in K562 cells impaired hemin-induced erythroid differentiation, assessed as hemoglobin accumulation, and inhibited GATA1 decline at both 24 (Figure 6E) and 48 h (Figures 6F and 6G). As the Ac-YVAD-CMK inhibitor may also inhibit CASP4, we used the CASP4 and

CASP5 inhibitor Ac-LEVD-CHO and found that it failed to affect the erythroid differentiation of K562 cells and their GATA1 amounts (Figure S6A).

CASP1 may target several proteins to regulate HSPC differentiation. One possibility is that CASP1 directly cleaves GATA1, as it has been reported for CASP3, which negatively regulates erythropoiesis through GATA1 cleavage (De Maria et al., 1999). Therefore, we studied whether recombinant human CASP1 was able to cleave human GATA1 *in vitro*. The results showed that recombinant CASP1 cleaved GATA1 generating N- and C-terminal proteolytic fragments of about 30 and 15 kDa, respectively (Figures S7A–S7C). CASP1 cleavage of GATA1 at residues D276 and/or D300 may generate the obtained fragments, so we obtained single and double CASP1 mutants (D276E and D300E) and found that CASP1 was only able to cleave GATA1 at residue D300 (Figure S7D). Collectively, all these results uncover an evolutionarily conserved role of the inflammasome in the regulation of erythroid versus myeloid fate decision and terminal erythroid differentiation via cleavage of GATA1.

Pharmacological Inhibition of the Inflammasome Rescues Zebrafish Models of Neutrophilic Inflammation and Anemia

Hematopoietic lineage bias is associated with chronic inflammatory diseases, cancer, and aging (Elias et al., 2017; Marzano et al., 2018; Wu et al., 2014). Neutrophilic dermatoses are a group of diseases characterized by the accumulation of neutrophils in the skin (Marzano et al., 2018). We used a zebrafish *Spint1a*-deficient line as model of neutrophilic dermatosis, since it is characterized by strong neutrophil infiltration into the skin (Carney et al., 2007; Mathias et al., 2007). It was found that *Spint1a*-deficient larvae had increased caspase-1 activity (Figure 7A) and an altered *spi1/gata1* ratio (Figure 7B). Notably, although pharmacological inhibition of caspase-1 failed to rescue neutrophil skin infiltration of *Spint1a*-deficient animals (Figures 7C and 7E), it was able to rescue their robust neutrophilia (Figures 7D and 7E). Similarly, genetic inactivation of *caspa* with CRISPR-Cas9 also rescued neutrophilia, but not neutrophil infiltration, of *Spint1a*-deficient animals (Figures 7F and 7G). However, CASP4 and CASP5 inhibition failed to rescue both neutrophilia and neutrophil infiltration in this animal model (Figure S6B).

We next model Diamond-Blackfan anemia, a ribosomopathy caused by inefficient translation of GATA1 (Danilova and Gazda, 2015), in zebrafish larvae by reducing *Gata1* amounts using a specific morpholino. We first titrated the morpholino and found that 1.7 ng/egg resulted in larvae with mild, moderate, and severe anemia (Figure 7H), while 0.85 ng/egg and 3.4 ng/egg had little or drastic effects, respectively (data not shown). We thus examined whether pharmacological inhibition of caspase-1 could rescue hemoglobin alterations of *Gata1*-deficient larvae. For these experiments, we treated larvae with the reversible inhibitor of caspase-1 Ac-YVAD-CHO for 24 to 48 hpf and analyzed hemoglobin at 72 hpf to allow terminal erythroid differentiation in the absence of caspase-1 inhibition. The results show that treatment of larvae for 24 h with this reversible inhibitor of caspase-1 partially rescued hemoglobin defects in *Gata1*-deficient larvae and *Spi1/Gata1* protein ratio (Figures 7I and 7J). These results taken together demonstrate that pharmacological inhibition of caspase-1 rescues hematopoietic lineage bias *in vivo*.

DISCUSSION

We report here an evolutionarily conserved signaling pathway that links the inflammasome with HSPC differentiation. Although previous reports have shown that proinflammatory signals are indispensable for HSPC emergence (Espin-Palazon et al., 2018), the roles of these signals, and in particular the inflammasome in HSPC formation, maintenance, and differentiation, are largely unknown. During periods of hematopoietic stress induced by chemotherapy or viral infection, activation of mouse NLRP1a prolongs cytopenia, bone-marrow hypoplasia, and immunosuppression (Masters et al., 2012). This effect is mediated by the CASP1-dependent, but ASC-independent, pyroptosis of hematopoietic progenitor cells (Masters et al., 2012). In addition, the NLRP3 inflammasome has been found to drive clonal expansion and pyroptotic cell death in myelodysplastic syndromes (Basiorka et al., 2016). Our results demonstrate that although the inflammasome is dispensable for HSPC emergence in zebrafish, it cell-intrinsically regulates HSPC differentiation in homeostasis conditions at two different levels: erythroid versus myeloid cell fate decision and terminal erythroid differentiation. Although CASP1 may target several proteins to regulate both processes, one plausible scenario is the cleavage of GATA1 at residue D300 by CASP1, which would result in the quick degradation of GATA1, since we were unable to detect processed GATA1 in zebrafish larvae or K562 cells. The rapid induction of GATA1 protein amounts in mouse HSC upon pharmacological inhibition of CASP1 supports this hypothesis. Although SPI1 protein amounts were unaffected by CASP1 inhibition in HSC, SPI1 expression will be reduced at later stages of differentiation, but as a consequence of reduced GM differentiation, not as a reason for it (Strasser et al., 2018). Our model is compatible with our recent report showing that the expression of SPI1 is not relevant for the erythroid versus myeloid switch, since sometimes is already downregulated or off when GATA1 expression starts but sometimes is still expressed (Hoppe et al., 2016; Strasser et al., 2018). However, once GATA1 starts to be expressed, the HSPC always differentiate into MegE with GATA1 high and SPI1 low or off (Hoppe et al., 2016). Therefore, reduced GATA1 amounts upon inflammasome activation lead to reduced erythropoiesis and thus increased myelopoiesis. At the same time, inflammatory signaling through tumor necrosis factor α (TNF α) and IL1- β has recently been shown to directly upregulate SPI1 protein directly in HSCs *in vitro* and *in vivo* (Etzrodt et al., 2018; Pietras et al., 2016).

Similarly, terminal erythroid differentiation also requires GATA1 cleavage by CASP1. Thus, we observed that pharmacological inhibition of CASP1 leads to GATA1 accumulation and altered erythroid differentiation of K562 cells. This is not unexpected, since GATA1 inhibits terminal erythroid differentiation *in vitro* (Whyatt et al., 1997) and *in vivo* (Whyatt et al., 2000). Although it remains to be elucidated the signals responsible for the activation of the inflammasome in erythroid versus myeloid cell fate decision and terminal erythroid differentiation, as well as the inflammasome components involved, our genetic studies in zebrafish show that Gbp4 and Asc are both intrinsically required *in vivo* by HSPC to regulate their differentiation. A mild activation of CASP1 is anticipated to avoid the pyroptotic cell death of hematopoietic cells. This may be achieved by the assembly of small ASC specks and/or the low abundance of caspase-1 in hematopoietic progenitor cells and

erythroid precursors, as occurs in neutrophils that exhibit sustained IL-1 β release without pyroptosis compared to macrophages (Boucher et al., 2018; Chen et al., 2014).

Hematopoietic lineage bias is associated to increased incidence of diseases with prominent inflammatory components, including atherosclerosis, autoimmunity, neurodegenerative disease and carcinogenesis (Elias et al., 2017). In particular, neutrophilic dermatosis is characterized by the accumulation of neutrophils in the skin and cutaneous lesions (Marzano et al., 2018). We observed that the robust neutrophilia of a zebrafish model of skin inflammation is reversed by pharmacological and genetic inhibition of Caspa, despite skin lesions and neutrophil infiltration are largely unaffected. Therefore, inflammasome activation alters granulopoiesis through reducing Gata1 expression and, more importantly, its pharmacological inhibition restores Gata1 amounts and neutrophil counts. Furthermore, the critical role of the inflammasome in the regulation of Gata1 has also been pointed out by the ability of pharmacological inhibition of Caspa to restore erythroid hemoglobin and Gata1 amounts, and to decline Spi 1 amounts, in a zebrafish model of reduced Gata1, as occurs in Diamond-Blackfan anemia (Danilova and Gazda, 2015). Collectively, all these results point out to the ability of inflammasome inhibition as a therapeutic approach to treat human diseases with associated hematopoietic lineage bias, such as neutrophilic inflammation (Marzano et al., 2018; Ray and Kolls, 2017), ACD (Weiss, 2015), and chemotherapy-induced anemia (Testa et al., 2015). The availability of an orally active CASP1 inhibitor, VX-765, with high specificity, excellent pharmacokinetic properties, and efficacy in rheumatoid arthritis and skin inflammation mouse models (Wannamaker et al., 2007), further supports the clinical testing of CASP1 inhibitors in hematopoietic lineage bias disorders.

STAR★METHODS

Detailed methods are provided in the online version of this paper and include the following:

CONTACT FOR REAGENT AND RESOURCE SHARING

Further information and requests for resources and reagents should be directed to and will be fulfilled by the Lead Contact, Victoriano Mulero (vmulero@um.es).

EXPERIMENTAL MODEL AND SUBJECT DETAILS

Zebrafish (*Danio rerio* H.) were obtained from the Zebrafish International Resource Center and mated, staged, raised and processed as described (Westerfield, 2000). The lines *roy^{a9/a9}*; *nacre^{w2/w2}* (*casper*) (White et al., 2008), *Tg(mpx:eGFP)^{j114}* (Renshaw et al., 2006), *Tg(mpeg1:eGFP)^{g22}*, *Tg(mpeg1:GAL4)^{g125}* (Ellett et al., 2011), *Tg(lyz:dsRED)^{nz50}* (Hall et al., 2007), *Tg(mpx:Gal4.VP16)^{j222}* (Davison et al., 2007), *Tg(lcr:eGFP)^{cz3325}* (Ganis et al., 2012), *Tg(runx1:GAL4)^{utn6}* (Tamplin et al., 2015), *T9(UAS:nfsB-mCherry)^{c264}* (Davison et al., 2007) and *Tg(spint1a)^{hi2217}* (Carney et al., 2007; Mathias et al., 2007) have been previously described. The experiments performed comply with the Guidelines of the European Union Council (Directive 2010/63/EU) and the Spanish RD 53/2013. Experiments and procedures were performed as approved by the Bioethical Committees of the University of Murcia (approval numbers #75/2014, #216/2014 and 395/2017).

Mouse experiments were performed with 12–16 week old, male, SPI1-eYFP and GATA1-mCherry reporter mice (C57BL/6J background). Animal experiments were approved according to Institutional guidelines of ETH Zurich and Swiss Federal Law by veterinary office of Canton Basel-Stadt, Switzerland (approval number #2655).

METHOD DETAILS

DNA Construct and Generation of Transgenics—The *uas:Asc CARD-GFP* construct was generated by MultiSite Gateway assemblies using LR Clonase II Plus (Life Technologies) according to standard protocols and using Tol2kit vectors described previously (Kwan et al., 2007). The expression constructs *Gbp4*, *Gbp4KS→AA*, *Gbp4 CARD*, *Gbp4KS→AA* and *CARD* (double mutant, DM) and *uas:gbp4KS→AA* (Tyrkalska et al., 2016); *Asc-Myc* and *Caspa* (Masumoto et al., 2003); and *Gcsfa* (Liongue et al., 2009) were previously described.

The line *Tg(UAS:gbp4KS→AA)^{ums3}* was previously described (Tyrkalska et al., 2016). *Tg(UAS:asc CARD-GFP)^{ums4}* was generated by microinjecting 0.5–1 cnl into the yolk sac of one-cell-stage embryos a solution containing 100 ng/μl *uas:asc CARD-GFP* and *uas:gbp4KS→AA* constructs, respectively, and 50 ng/μl Tol2 RNA in microinjection buffer (× 0.5 Tango buffer and 0.05% phenol red solution) using a microinjector (Narishige).

Morpholino, RNA and Protein Injection and Chemical Treatments of Zebrafish Larvae—Specific morpholinos (Gene Tools) were resuspended in nuclease-free water at 1 mM (Table S1). *In vitro*-transcribed RNA was obtained following the manufacturer's instructions (mMESSAGE mMACHINE kit, Ambion). Morpholinos and RNA were mixed in microinjection buffer and microinjected into the yolk sac of one-cell-stage embryos using a microinjector (Narishige) (0.5–1 nL per embryo). The same amount of MOs and/or RNA was used in all experimental groups.

For genetic inactivation of *caspa*, injection mixes were prepared with 500 ng/μl EnGen® Cas9 NLS from *Streptococcus pyogenes* and 100 ng/μl *tracrRNA* with negative control or *caspa* (5'-GAACCAATTC CGAAGGATCC-') crRNAs in 300 mM KCl buffer, incubated for 5 min at 37°C and used directly without further storage (Burger et al., 2016).

In some experiments, 1–2 dpf embryos were manually dechorionated and treated for 1 to 3 dpf at 28°C by bath immersion with the caspase-1 inhibitors Ac-YVAD-CMK (irreversible) or Ac-YVAD-CHO (reversible), and the reversible caspase-4 and caspase-5 inhibitor Ac-LEVD-CHO (100 μM, Peptanova) diluted in egg water supplemented with 1% DMSO or with Metronidazole (Mtz, 5 mM, Sigma-Aldrich).

Live Imaging, Sudan Black Staining of Neutrophils, Neutrophil Ablation and Erythrocyte Determination in Zebrafish Larvae—At 48 and 72 hpf, larvae were anesthetized in tricaine and mounted in 1% (wt/vol) low-melting-point agarose (Sigma-Aldrich) dissolved in egg water (de Oliveira et al., 2013). Images were captured with an epifluorescence Lumar V12 stereomicroscope equipped with green and red fluorescent filters while animals were kept in their agar matrixes at 28.5°C. All images were acquired

with the integrated camera on the stereomicroscope and were used for subsequently counting the total number of neutrophils, macrophages or HSPC in whole larvae.

In order to decrease pigmentation and improve the signal from Sudan black staining, 24 hpf larvae were incubated in 200 mM 1-phenyl 2-thiourea (PTU) until 72 hpf, when they were anesthetized in buffered tricaine and fixed overnight at 4°C in 4% methanol-free formaldehyde. On the next day, all the larvae were rinsed with PBS thrice, incubated for 15 min with Sudan black and washed extensively in 70% EtOH in water. After that a progressive rehydration was performed: 50% EtOH in PBS and 0.1% Tween 20 (PBT) (Sigma-Aldrich), 25% EtOH in PBT and PBT alone. Finally, the larvae were visualized immediately using a Scope.AI stereomicroscope equipped with a digital camera (AxioCam ICc 3, Zeiss) (Le Guyader et al., 2008).

For neutrophil ablation, larvae *Tg(mpx:Gal4.VP16; UAS:nsfb-mCherry)* were treated at 2 dpf with 5 mM Mtz and kept in dark. At 72 hpf the drug was removed and larvae were treated up to 7 dpf with 1% DMSO alone or containing Ac-YVAD-CMK (100 µM). The inhibitor was refreshed every 24 h and the larvae were imaged once a day up to 7 dpf and the number of neutrophils determined (Davison et al., 2007; Halpern et al., 2008).

Erythrocyte counts were determined by flow cytometry. At 3 dpf, pools of 50 *Tg(lcr:eGFP)* larvae were anesthetized in tricaine, minced with a razor blade and incubated at 28°C for 30 min with 0.077 mg/mL Liberase (Roche). Afterward, 10% FBS in PBS was added to inactivate liberase and the resulting cell suspension passed through a 40 µm cell strainer. Flow cytometric acquisitions were performed on a FACSCALIBUR (BD) and analysis was based on forward scatter and side scatter, duplicate exclusion, exclusion of dead cells by addition of SYTOX Blue to a final concentration of 1 µM, and GFP fluorescence. Before analyzing *Tg(lcr:eGFP)* zebrafish cell suspensions, the flow cytometry gates were set with suspensions from the same number of 3-dpf GFP-negative wild-type larvae of the same background. Analyses were performed using FlowJo software (Treestar).

Infection Assays of Zebrafish Larvae—For infection experiments, *Salmonella enterica* serovar Typhimurium strain 12023 (wild-type) provided by Prof. Holden was used. Overnight cultures in Luria-Bertani medium (LB) were diluted 1/5 in LB with 0.3 M NaCl, incubated at 37°C until 1.5 optical density at 600 nm was reached, and finally diluted in sterile PBS. Larvae of 2 dpf were anesthetized in embryo medium with 0.16 mg/mL tricaine and 10 bacteria were injected into the yolk sac or otic vesicle. Larvae were allowed to recover in egg water at 28–29°C, and monitored for clinical signs of disease or mortality over 5 days and neutrophil recruitment up to 24 hpi (Tyrkalska et al., 2016).

Whole-Mount RNA *In Situ* Hybridization (WISH) in Zebrafish Larvae—Transparent Casper embryos were used for WISH (Thisse et al., 1993). *gatala*, *spilb*, *gcsfr*, *cmyb*, *runxl* and *ragl* sense and antisense RNA probes were generated using the DIG RNA Labeling Kit (Roche Applied Science) from linearized plasmids. Embryos were imaged using a Scope.AI stereomicroscope equipped with a digital camera (AxioCam ICc 3, Zeiss).

K562 Cell Culture and Erythroid Differentiation Assays—K562 cells were maintained in RPMI supplemented with 10% FCS, 2 mM Glutamin, and 1% penicillin-streptomycin. Cells were maintained and split before confluence every 72h. For the differentiation, cells were treated with 50 mM hemin, prepared as previously described (Smith et al., 2000), in the presence of 0.1% DMSO alone or containing 100 μ M Ac-YVAD-CMK or Ac-LEVD-CHO. Cells were collected at different time points (0, 6, 12, 24, 48 hours post-hemin addition), centrifuged, washed with PBS and stored at -80° C.

Caspase-1 Activity Assay—The caspase-1 activity was determined with the fluorometric substrate Z-YVAD-AFC as described previously (Angosto et al., 2012; Lopez-Castejon et al., 2008; Tyrkalska et al., 2016). In brief, 30 pooled zebrafish larvae and 8×10^5 K562 cells were lysed in hypotonic cell lysis buffer [25 mM 4-(2-hydroxyethyl)piperazine-1-ethanesulfonic acid (HEPES), 5 mM ethylene glycol-bis(2-aminoethylether)-N,N,N',N'-tetraacetic acid (EGTA), 5 mM dithiothreitol (DTT), 1:20 protease inhibitor cocktail, pH 7.5] on ice for 10 min. For each reaction, 80 μ g protein were incubated for 90 min at 23° C with 50 μ M Z-YVAD-AFC and 50 μ l of reaction buffer [0.2% 3-[(3-cholamidopropyl)dimethylammonio]-1-propanesulfonate (CHAPS), 0.2 M HEPES, 20% sucrose, 29 mM DTT, pH 7.5]. After the incubation, the fluorescence of the AFC released from the Z-YVAD-AFC substrate was measured with a FLUOstart spectofluorometer (BGM, LabTechnologies) at an excitation wavelength of 405 nm and an emission wavelength of 492 nm. One representative caspase-1 activity assay out of the three carried out is shown accompanying each cell count.

Laser Confocal Microscopy—Cells were seeded in Poly-L-Lys Cellware 12mm cover (Corning), 50,000 cells in 100 μ l were allowed to attach to the cover during 10 min at room temperature, then medium and treatment were added. After hemin treatment cells were washed with PBS, fixed with 4% paraformaldehyde in PBS 10 min, incubated 20 min at room temperature with 20 mM glycine, permeabilized with 0.5% NP40 and blocked for 1 h with 2% BSA. Cells were then labeled with corresponding primary antibody, followed by Alexa 568-conjugated secondary antibody (Thermo Fisher Scientific). Samples were mounted using a mounting medium from Dako and examined with a Leica laser scanning confocal microscope AOBS and software (Leica Microsystems). The images were acquired in a $1,024 \times 1,024$ pixel format in sequential scan mode between frames to avoid cross-talk. The objective used was HCX PL APO CS $\times 63$ and the pinhole value was 1, corresponding to 114.73 μ m.

Immunoblotting—Lysis buffer for mammalian cell lysis contained 50 mM Tris-HCl (pH 7.5), 150 mM NaCl, 1 mM EDTA, 1 mM EGTA, 1% (w/v) NP-40 and fresh protease inhibitor (1/20, P8340, Sigma-Aldrich), while for zebrafish larvae lysis contained 1% SDS. Protein quantification was done with BCA kit using BSA as a standard. Cell lysates (40 μ g) in SDS sample buffer were subjected to electrophoresis on a polyacrylamide gel and transferred to PVDF membranes. The membranes were incubated for 1 h with TTBS containing 5% (w/v) skimmed dried milk powder or 2% (w/v) BSA. The membranes were immunoblotted in the same buffer 16 h at 4° C with the indicated primary antibodies. The blots were then washed with TTBS and incubated for 1 h at room temperature with

secondary HRP-conjugated antibodies diluted 2,500-fold in 5% (w/v) skimmed milk in TTBS. After repeated washes, the signal was detected with the enhanced chemiluminescence reagent and ChemiDoc XRS Biorad. The primary antibodies used are: rabbit polyclonal to human GATA1 (1/200, #sc1234, Santa Cruz Biotechnology) for confocal assay, rabbit mAb to human GATA1 (1/200, #3535, Cell Signaling) for immunoblotting, rabbit polyclonal to CASP1 (1/200, #sc56036 Santa Cruz Biotechnology) for confocal assay, rabbit polyclonal to zebrafish Gata1a and Spi1b (1/2000, #GTX128333 and GTX128266, GeneTex), rabbit polyclonal to histone H3 (1/200, #ab1791, Abcam) and Monoclonal ANTI-FLAG® M2-Peroxidase (HRP) antibody produced in mouse. Densitometry analysis has been performed using Fiji ImageJ software (Schindelin et al., 2012).

Immunoprecipitation and Recombinant Caspase-1 Assay—Pull down assays were also performed as described previously (Tyrkalska et al., 2017), with small modifications. Cells were washed twice with PBS, solubilized in lysis buffer (50 mM Tris-HCl, pH 7.7, 150 mM NaCl, 1% NP-40 and 1:20 protease inhibitor cocktail) during 30 min in agitation and centrifuged (13,000 × g, 10 min). Cell lysate (1 mg) was incubated for 2 h at 4°C under gentle agitation with 40 ml of slurry of ANTI-FLAG® M2. The immunoprecipitates were washed four times with lysis buffer containing 0.15 M NaCl, washed twice with PBS and incubated with 10 IU recombinant caspase-1 in reaction buffer (50 mM HEPES, pH 7.2, 50mM NaCl, 0.1% Chaps, 10 mM EDTA, 5% Glycerol, and 10 mM DTT) during 2 h at 37°C. The resin was boiled in SDS sample buffer 5 min at 95°C and the bound proteins were resolved on 4%–15% SDS-PAGE and transferred to PVDF membranes for 1h at 300 mA. Blots were probed with antibodies to FLAG and GATA1 (see above).

Analysis of Gene Expression—Total RNA was extracted from 10⁶ K562 cells, whole embryos or larvae (60) or larval tails (100) with TRIzol reagent (Thermo Fisher Scientific) following the manufacturer's instructions and treated with DNase I, amplification grade (1 U/mg RNA; Invitrogen). SuperScript III RNase H⁻ Reverse Transcriptase (Invitrogen) was used to synthesize first-strand cDNA with oligo(dT)18 primer from 1 µg of total RNA at 50°C for 50 min. Real-time PCR was performed with an ABI PRISM 7500 instrument (Applied Biosystems) using Power SYBR Green Master Mix. Reaction mixtures were incubated for 10 min at 95°C, followed by 40 cycles of 15 s at 95°C, 1 min at 60°C, and finally 15 s at 95°C, 1 min 60°C and 15 s at 95°C. For each mRNA, gene expression was normalized to the ribosomal protein S11 (*rps11*) for zebrafish or β-actin (*ACTB*) for human cells content in each sample following the Pfaffl method (Pfaffl, 2001). The primers used are shown in (Table S2). In all cases, each PCR was performed with triplicate samples and repeated with at least two independent samples.

Isolation of Mouse HSCs—Male SPI1-eYFP and GATA1-mCherry mice were euthanized and isolation of HSCs was performed according to previously described protocols (Cabezas-Wallscheid et al., 2014; Hoppe et al., 2016; Kiel et al., 2005). Briefly, femurs, tibiae and vertebrae of adult mice were isolated and crushed in FACS buffer (2% FCS (PAA) + 1mM EDTA in PBS). Bone marrow suspension was subjected to ACK lysing buffer for 2 min followed by lineage depletion steps including incubation with biotinylated

antibodies cocktail of CD3e, CD19, B220, CD11b, Gr-1 and Ter-119 for 7 min, streptavidin-conjugated beads (Roche) for 7 min and immune-magnetic (Stem Cell Technologies) separation for 7 min. Lineage depleted cells were stained with color-conjugated primary antibodies for 90 min. FACS sorting of HSCs was performed on FACS ARIA III (BD Biosciences) using the Lineage⁻ Sca1⁺ cKit⁺ CD34⁻ CD48⁻ CD135⁻ CD150⁺. All steps were performed at 4°C.

Mouse Single-Cell Liquid Culture Colony Assay—Single-cell sort of HSCs was performed in plastic-bottom 384 well plates (Greiner Bio-one) using FACS ARIA III under standard permissive culture media (IMDM (GIBCO) + 5% BIT (Stem Cell Technologies) + P/S + SCF + Epo + Tpo + IL3 + IL6) with or without 100 μM Ac-YVAD-CMK. Plates were incubated at 37°C and 5% CO₂. At day 8, color-conjugated antibodies against lineage markers (CD41-APC + CD16/32-BV421) were added (1:5000 dilution) in wells, incubated for 3 hours at 37°C and 5% CO₂ and imaging of hematopoietic colonies was performed on Nikon Eclipse Ti-E microscope. Colonies were scored manually. Granulocyte-monocyte colonies were indicated by morphology, CD16/32 and SPI-eYFP expression while megakaryocyte-erythrocyte colonies were indicated by morphology, CD41 and GATA1-mCherry expression as previously described (Hoppe et al., 2016).

Time-Lapse Imaging of Mouse HSCs—HSCs were sorted using FACS ARIA III and seeded in plastic-bottom 384 well plates (Greiner Bio-one) in multi-lineage supporting culture media as described (Hoppe et al., 2016) (IMDM + 5% BIT + P/S + SCF + Epo + Tpo + IL3 + IL6) with or without 100mM Ac-YVAD-CMK. Time-lapse imaging and quantification of SPI1-eYFP and GATA1-mCherry in HSCs was performed using previously established protocols (Etzrodt et al., 2018; Hilsenbeck et al., 2017; Hilsenbeck et al., 2016; Hoppe et al., 2016).

Quantification and Statistical Analysis—Data are shown as mean ± SEM and were analyzed by analysis of variance (ANOVA) and a Tukey or Bonferroni multiple range test to determine differences among groups. The differences between two samples were analyzed by the Student t test. Fisher's exact and Chi-square tests were used for the analysis of contingency tables. A log rank test with the Bonferroni correction for multiple comparisons was used to calculate the statistical differences in the survival of the different experimental groups.

Supplementary Material

Refer to Web version on PubMed Central for supplementary material.

ACKNOWLEDGMENTS

We strongly acknowledge I. Fuentes and P. Martinez for their excellent technical assistance with the zebrafish experiments. We also thank Profs.

S.A. Renshaw, P. Crosier, G. Lieschke, M. Hammerschmidt, and M. Halpern for the zebrafish lines, N. Inohara for the zebrafish Asc-Myc and Caspa constructs, C. Hall for the zebrafish Gcsfa construct, D. Holden for the ST strain, and P. Pelegrin and A. Baroja-Mazo for critical reading of the manuscript. This work was supported by the Spanish Ministry of Science, Innovation and Universities (grants BIO2014-52655-R and BIO2017-84702-R to V.M. and PI13/0234 to M.L.C., PhD fellowship to F.J.M.-M. and Juan de la Cierva postdoctoral contract to F.A.-P.), all co-

funded with Fondos Europeos de Desarrollo Regional/European Regional Development Funds), Fundacion Seneca-Murcia (grant 19400/PI/14 to M.L.C.), the University of Murcia (postdoctoral contracts to A.B.-P.O. and D.G.-M., and PhD fellowship to F.J.M.-M.), SNF grant 179490 to T.S., and the European 7th Framework Initial Training Network Fish For Pharma (PhD fellowship to S.D.T., PITG-GA-2011-289209). The funders had no role in study design, data collection and analysis, decision to publish, or preparation of the manuscript.

DECLARATION OF INTEREST

L.I.Z. is a founder and stockholder of Fate Therapeutics, Inc., Scholar Rock, and Camp4 Therapeutics. A patent for the use of caspase-1 inhibitors to treat anemia has been registered by Universidad de Murcia, Boston Children's Hospital and Instituto Murciano de Investigación Biosanitaria (#P201831288).

REFERENCES

- Andersson LC, Nilsson K, and Gahmberg CG (1979). K562-a human erythroleukemic cell line. *Int. J. Cancer* 23, 143–147. [PubMed: 367973]
- Angosto D, López-Castejón G, López-Muñoz A, Sepulcre MP, Arizcun M, Meseguer J, and Mulero V. (2012). Evolution of inflammasome functions in vertebrates: Inflammasome and caspase-1 trigger fish macrophage cell death but are dispensable for the processing of IL-1 p. *Innate Immun.* 18, 815–824. [PubMed: 22456941]
- Basiorka AA, McGraw KL, Eksioglu EA, Chen X, Johnson J, Zhang L, Zhang Q, Irvine BA, Cluzeau T, Sallman DA, et al. (2016). The NLRP3 inflammasome functions as a driver of the myelodysplastic syndrome phenotype. *Blood* 128, 2960–2975. [PubMed: 27737891]
- Berman J, Payne E, and Hall C. (2012). The zebrafish as a tool to study hematopoiesis, human blood diseases, and immune function. *Adv. Hematol.* 2012, 425345.
- Birbrair A, and Frenette PS (2016). Niche heterogeneity in the bone marrow. *Ann. N Y Acad. Sci.* 1370, 82–96. [PubMed: 27015419]
- Boucher D, Monteleone M, Coll RC, Chen KW, Ross CM, Teo JL, Gomez GA, Holley CL, Bierschenk D, Stacey KJ, et al. (2018). Caspase-1 self-cleavage is an intrinsic mechanism to terminate inflammasome activity. *J. Exp. Med.* 215, 827–840. [PubMed: 29432122]
- Broz P, and Monack DM (2011). Molecular mechanisms of inflammasome activation during microbial infections. *Immunol. Rev.* 243, 174–190. [PubMed: 21884176]
- Burger A, Lindsay H, Felker A, Hess C, Anders C, Chiavacci E, Zaugg J, Weber LM, Catena R, Jinek M, et al. (2016). Maximizing mutagenesis with solubilized CRISPR-Cas9 ribonucleoprotein complexes. *Development* 143, 2025–2037. [PubMed: 27130213]
- Burns CE, Traver D, Mayhall E, Shepard JL, and Zon LI (2005). Hematopoietic stem cell fate is established by the Notch-Runx pathway. *Genes Dev.* 19, 2331–2342. [PubMed: 16166372]
- Cabezas-Wallscheid N, Klimmeck D, Hansson J, Lipka DB, Reyes A, Wang Q, Weichenhan D, Lier A, von Paleske L, Renders S, et al. (2014). Identification of regulatory networks in HSCs and their immediate progeny via integrated proteome, transcriptome, and DNA methylome analysis. *Cell Stem Cell* 15, 507–522. [PubMed: 25158935]
- Cantor AB, and Orkin SH (2002). Transcriptional regulation of erythropoiesis: an affair involving multiple partners. *Oncogene* 21, 3368–3376. [PubMed: 12032775]
- Carney TJ, von der Hardt S, Sonntag C, Amsterdam A, Topczewski J, Hopkins N, and Hammerschmidt M. (2007). Inactivation of serine protease Matriptase 1a by its inhibitor Hai1 is required for epithelial integrity of the zebrafish epidermis. *Development* 134, 3461–3471. [PubMed: 17728346]
- Chen KW, Groß CJ, Sotomayor FV, Stacey KJ, Tschopp J, Sweet MJ, and Schroder K. (2014). The neutrophil NLR4 inflammasome selectively promotes IL-1 β maturation without pyroptosis during acute Salmonella challenge. *Cell Rep.* 8, 570–582. [PubMed: 25043180]
- Cumano A, and Godin I. (2007). Ontogeny of the hematopoietic system. *Annu. Rev. Immunol.* 25, 745–785. [PubMed: 17201678]
- Curado S, Anderson RM, Jungblut B, Mumm J, Schroeter E, and Stainier DY (2007). Conditional targeted cell ablation in zebrafish: a new tool for regeneration studies. *Dev. Dyn.* 236, 1025–1035. [PubMed: 17326133]

- Curado S, Stainier DY, and Anderson RM (2008). Nitroreductase-mediated cell/tissue ablation in zebrafish: a spatially and temporally controlled ablation method with applications in developmental and regeneration studies. *Nat. Protoc.* 3, 948–954. [PubMed: 18536643]
- Danilova N, and Gazda HT (2015). Ribosomopathies: how a common root can cause a tree of pathologies. *Dis. Model. Mech.* 8, 1013–1026. [PubMed: 26398160]
- Davison JM, Akitake CM, Goll MG, Rhee JM, Gosse N, Baier H, Halpern ME, Leach SD, and Parsons MJ (2007). Transactivation from Gal4-VP16 transgenic insertions for tissue-specific cell labeling and ablation in zebrafish. *Dev. Biol.* 304, 811–824. [PubMed: 17335798]
- De Maria R, Zeuner A, Eramo A, Domenichelli C, Bonci D, Grignani F, Srinivasula SM, Alnemri ES, Testa U, and Peschle C. (1999). Negative regulation of erythropoiesis by caspase-mediated cleavage of GATA-1. *Nature* 401, 489–493. [PubMed: 10519553]
- de Oliveira S, Reyes-Aldasoro CC, Candel S, Renshaw SA, Mulero V, and Calado A. (2013). Cxcl8 (IL-8) mediates neutrophil recruitment and behavior in the zebrafish inflammatory response. *J. Immunol.* 190,4349–4359. [PubMed: 23509368]
- Elias HK, Bryder D, and Park CY (2017). Molecular mechanisms underlying lineage bias in aging hematopoiesis. *Semin. Hematol.* 54, 4–11. [PubMed: 28088987]
- Ellett F, and Lieschke GJ (2010). Zebrafish as a model for vertebrate hematopoiesis. *Curr. Opin. Pharmacol.* 10, 563–570. [PubMed: 20538521]
- Ellett F, Pase L, Hayman JW, Andrianopoulos A, and Lieschke GJ (2011). mpeg1 promoter transgenes direct macrophage-lineage expression in zebrafish. *Blood* 117, e49–e56. [PubMed: 21084707]
- Espin-Palazon R, Weijts B, Mulero V, and Traver D. (2018). Proinflammatory Signals as Fuel for the Fire of Hematopoietic Stem Cell Emergence. *Trends Cell Biol.* 28, 58–66. [PubMed: 28882414]
- Etzrodt M, Ahmed N, Hoppe PS, Loeffler D, Skylaki S, Hilsenbeck O, Kokkaliaris KD, Kaltenbach HM, Stelling J, Nerlov C, and Schroeder T. (2018). Inflammatory signals directly instruct PU.1 in HSCs via TNF. *Blood* 133, 816–819. [PubMed: 30301719]
- Ferreira R, Ohneda K, Yamamoto M, and Philipsen S. (2005). GATA1 function, a paradigm for transcription factors in hematopoiesis. *Mol. Cell. Biol.* 25, 1215–1227. [PubMed: 15684376]
- Ganis JJ, Hsia N, Trompouki E, de Jong JL, DiBiase A, Lambert JS, Jia Z, Sabo PJ, Weaver M, Sandstrom R, et al. (2012). Zebrafish globin switching occurs in two developmental stages and is controlled by the LCR. *Dev. Biol.* 366, 185–194. [PubMed: 22537494]
- Gore AV, Pillay LM, Venero Galanternik M, and Weinstein BM (2018). The zebrafish: A fantastic model for hematopoietic development and disease. *Wiley Interdiscip. Rev. Dev. Biol.* 7, e312. [PubMed: 29436122]
- Hall C, Flores MV, Storm T, Crosier K, and Crosier P. (2007). The zebrafish lysozyme C promoter drives myeloid-specific expression in transgenic fish. *BMC Dev. Biol.* 7, 42. [PubMed: 17477879]
- Hall CJ, Flores MV, Oehlers SH, Sanderson LE, Lam EY, Crosier KE, and Crosier PS (2012). Infection-responsive expansion of the hematopoietic stem and progenitor cell compartment in zebrafish is dependent upon inducible nitric oxide. *Cell Stem Cell* 7, 198–209.
- Halpern ME, Rhee J, Goll MG, Akitake CM, Parsons M, and Leach SD (2008). Gal4/UAS transgenic tools and their application to zebrafish. *Zebrafish* 5, 97–110. [PubMed: 18554173]
- Hilsenbeck O, Schwarzfischer M, Skylaki S, Schauburger B, Hoppe PS, Loeffler D, Kokkaliaris KD, Hastreiter S, Skylaki E, Filipczyk A, et al. (2016). Software tools for single-cell tracking and quantification of cellular and molecular properties. *Nat. Biotechnol.* 34, 703–706. [PubMed: 27404877]
- Hilsenbeck O, Schwarzfischer M, Loeffler D, Dimopoulos S, Hastreiter S, Marr C, Theis FJ, and Schroeder T. (2017). fastER: a user-friendly tool for ultrafast and robust cell segmentation in large-scale microscopy. *Bioinformatics* 33, 2020–2028. [PubMed: 28334115]
- Hoppe PS, Schwarzfischer M, Loeffler D, Kokkaliaris KD, Hilsenbeck O, Moritz N, Ende M, Filipczyk A, Gambardella A, Ahmed N, et al. (2016). Early myeloid lineage choice is not initiated by random PU.1 to GATA1 protein ratios. *Nature* 535, 299–302. [PubMed: 27411635]
- Jagannathan-Bogdan M, and Zon LI (2013). Hematopoiesis. *Development* 140, 2463–2467. [PubMed: 23715539]

- Kiel MJ, Yilmaz OH, Iwashita T, Yilmaz OH, Terhorst C, and Morrison SJ (2005). SLAM family receptors distinguish hematopoietic stem and progenitor cells and reveal endothelial niches for stem cells. *Cell* 121, 1109–1121. [PubMed: 15989959]
- Koeffler HP, and Golde DW (1980). Human myeloid leukemia cell lines: a review. *Blood* 56, 344–350. [PubMed: 6996765]
- Kondo M (2010). Lymphoid and myeloid lineage commitment in multipotent hematopoietic progenitors. *Immunol. Rev.* 238, 37–46. [PubMed: 20969583]
- Kondo M, Wagers AJ, Manz MG, Prohaska SS, Scherer DC, Beilhack GF, Shizuru JA, and Weissman IL (2003). Biology of hematopoietic stem cells and progenitors: implications for clinical application. *Annu. Rev. Immunol.* 21, 759–806. [PubMed: 12615892]
- Kuri P, Schieber NL, Thumberger T, Wittbrodt J, Schwab Y, and Leptin M. (2017). Dynamics of in vivo ASC speck formation. *J. Cell Biol.* 216, 2891–2909. [PubMed: 28701426]
- Kwan KM, Fujimoto E, Grabher C, Mangum BD, Hardy ME, Campbell DS, Parant JM, Yost HJ, Kanki JP, and Chien CB (2007). The Tol2kit: a multisite gateway-based construction kit for Tol2 transposon transgenesis constructs. *Dev. Dyn.* 236, 3088–3099. [PubMed: 17937395]
- Lamkanfi M, and Dixit VM (2014). Mechanisms and functions of inflammasomes. *Cell* 157, 1013–1022. [PubMed: 24855941]
- Latz E, Xiao TS, and Stutz A. (2013). Activation and regulation of the inflammasomes. *Nat. Rev. Immunol.* 13, 397–411. [PubMed: 23702978]
- Le Guyader D, Redd MJ, Colucci-Guyon E, Murayama E, Kissa K, Briolat V, Mordelet E, Zapata A, Shinomiya H, and Herbomel P. (2008). Origins and unconventional behavior of neutrophils in developing zebrafish. *Blood* 111, 132–141. [PubMed: 17875807]
- Liongue C, Hall CJ, O’Connell BA, Crosier P, and Ward AC (2009). Zebrafish granulocyte colony-stimulating factor receptor signaling promotes myelopoiesis and myeloid cell migration. *Blood* 113, 2535–2546. [PubMed: 19139076]
- López-Castejón G, Sepulcre MP, Mulero I, Pelegrín P, Meseguer J, and Mulero V. (2008). Molecular and functional characterization of gilthead seabream *Sparus aurata* caspase-1: the first identification of an inflammatory caspase in fish. *Mol. Immunol.* 45, 49–57. [PubMed: 17610954]
- Martinon F, Mayor A, and Tschopp J. (2009). The inflammasomes: guardians of the body. *Annu. Rev. Immunol.* 27, 229–265. [PubMed: 19302040]
- Marzano AV, Borghi A, Wallach D, and Cugno M (2018). A Comprehensive Review of Neutrophilic Diseases. *Clin. Rev. Allergy Immunol.* 54, 114–130. [PubMed: 28688013]
- Masters SL, Gerlic M, Metcalf D, Preston S, Pellegrini M, O’Donnell JA, McArthur K, Baldwin TM, Chevrier S, Nowell CJ, et al. (2012). NLRP1 inflammasome activation induces pyroptosis of hematopoietic progenitor cells. *Immunity* 37, 1009–1023. [PubMed: 23219391]
- Masumoto J, Zhou W, Chen FF, Su F, Kuwada JY, Hidaka E, Katsuyama T, Sagara J, Taniguchi S, Ngo-Hazelett P, et al. (2003). Caspy, a zebrafish caspase, activated by ASC oligomerization is required for pharyngeal arch development. *J. Biol. Chem.* 278, 4268–4276. [PubMed: 12464617]
- Mathias JR, Dodd ME, Walters KB, Rhodes J, Kanki JP, Look AT, and Huttenlocher A. (2007). Live imaging of chronic inflammation caused by mutation of zebrafish Hai1. *J. Cell Sci.* 120, 3372–3383. [PubMed: 17881499]
- Morrison SJ, Shah NM, and Anderson DJ (1997). Regulatory mechanisms in stem cell biology. *Cell* 88, 287–298. [PubMed: 9039255]
- Nerlov C, Querfurth E, Kulesa H, and Graf T. (2000). GATA-1 interacts with the myeloid PU.1 transcription factor and represses PU.1-dependent transcription. *Blood* 95, 2543–2551. [PubMed: 10753833]
- Pfaffl MW (2001). A new mathematical model for relative quantification in real-time RT-PCR. *Nucleic Acids Res.* 29, e45. [PubMed: 11328886]
- Pietras EM, Mirantes-Barbeito C, Fong S, Loeffler D, Kovtonyuk LV, Zhang S, Lakshminarasimhan R, Chin CP, Techner JM, Will B, et al. (2016). Chronic interleukin-1 exposure drives haematopoietic stem cells towards precocious myeloid differentiation at the expense of self-renewal. *Nat. Cell Biol.* 18, 607–618. [PubMed: 27111842]

- Pilla DM, Hagar JA, Haldar AK, Mason AK, Degrandi D, Pfeffer K, Ernst RK, Yamamoto M, Miao EA, and Coers J. (2014). Guanylate binding proteins promote caspase-11-dependent pyroptosis in response to cytoplasmic LPS. *Proc. Natl. Acad. Sci. USA* 111, 6046–6051. [PubMed: 24715728]
- Prajsnar TK, Hamilton R, Garcia-Lara J, McVicker G, Williams A, Boots M, Foster SJ, and Renshaw SA (2012). A privileged intraphagocyte niche is responsible for disseminated infection of *Staphylococcus aureus* in a zebrafish model. *Cell. Microbiol.* 14, 1600–1619. [PubMed: 22694745]
- Rathinam VA, and Fitzgerald KA (2016). Inflammasome Complexes: Emerging Mechanisms and Effector Functions. *Cell* 166, 792–800.
- Ray A, and Kolls JK (2017). Neutrophilic Inflammation in Asthma and Association with Disease Severity. *Trends Immunol.* 38, 942–954. [PubMed: 28784414]
- Rekhtman N, Radparvar F, Evans T, and Skoultschi AI (1999). Direct interaction of hematopoietic transcription factors PU.1 and GATA-1: functional antagonism in erythroid cells. *Genes Dev.* 13, 1398–1411. [PubMed: 10364157]
- Renshaw SA, Loynes CA, Trushell DM, Elworthy S, Ingham PW, and Whyte MK (2006). Atransgenic zebrafish model of neutrophilic inflammation. *Blood* 108, 3976–3978. [PubMed: 16926288]
- Santos JC, Dick MS, Lagrange B, Degrandi D, Pfeffer K, Yamamoto M, Meunier E, Pelczar P, Henry T, and Broz P (2018). LPS targets host guanylate-binding proteins to the bacterial outer membrane for non-canonical inflammasome activation. *EMBO J.* 37, e98089.
- Schindelin J, Arganda-Carreras I, Frise E, Kaynig V, Longair M, Pietzsch T, Preibisch S, Rueden C, Saalfeld S, Schmid B, et al. (2012). Fiji: an open-source platform for biological-image analysis. *Nat. Methods* 9, 676–682. [PubMed: 22743772]
- Sharma D, and Kanneganti TD (2016). The cell biology of inflammasomes: Mechanisms of inflammasome activation and regulation. *J. Cell Biol.* 213, 617–629. [PubMed: 27325789]
- Smith RD, Malley JD, and Schechter AN (2000). Quantitative analysis of globin gene induction in single human erythroleukemic cells. *Nucleic Acids Res.* 28, 4998–5004. [PubMed: 11121491]
- Stachura DL, Svoboda O, Campbell CA, Espín-Palazón R, Lau RP, Zon LI, Bartunek P, and Traver D. (2013). The zebrafish granulocyte colony-stimulating factors (Gcsfs): 2 paralogous cytokines and their roles in hematopoietic development and maintenance. *Blood* 122, 3918–3928. [PubMed: 24128862]
- Strasser MK, Hoppe PS, Loeffler D, Kokkaliaris KD, Schroeder T, Theis FJ, and Marr C. (2018). Lineage marker synchrony in hematopoietic genealogies refutes the PU.1/GATA1 toggle switch paradigm. *Nat. Commun.* 9, 2697. [PubMed: 30002371]
- Tamplin OJ, Durand EM, Carr LA, Childs SJ, Hagedorn EJ, Li P, Yzaguirre AD, Speck NA, and Zon LI (2015). Hematopoietic stem cell arrival triggers dynamic remodeling of the perivascular niche. *Cell* 160, 241–252. [PubMed: 25594182]
- Testa U, Castelli G, and Elvira P. (2015). Experimental and investigational therapies for chemotherapy-induced anemia. *Expert Opin. Investig. Drugs* 24, 1433–1445.
- Thisse C, Thisse B, Schilling TF, and Postlethwait JH (1993). Structure of the zebrafish *snail1* gene and its expression in wild-type, spadetail and no tail mutant embryos. *Development* 119, 1203–1215. [PubMed: 8306883]
- Tyrkalska SD, Candel S, Angosto D, Gómez-Abellan V, Martín-Sánchez F, García-Moreno D, Zapata-Perez R, Sanchez-Ferrer A, Sepulcre MP, Pelegrín P, and Mulero V. (2016). Neutrophils mediate *Salmonella Typhimurium* clearance through the GBP4 inflammasome-dependent production of prostaglandins. *Nat. Commun.* 7, 12077. [PubMed: 27363812]
- Tyrkalska SD, Candel S, Pérez-Oliva AB, Valera A, Alcaraz-Pérez F, García-Moreno D, Cayuela ML, and Mulero V. (2017). Identification of an Evolutionarily Conserved Ankyrin Domain-Containing Protein, Caiap, Which Regulates Inflammasome-Dependent Resistance to Bacterial Infection. *Front. Immunol.* 8, 1375. [PubMed: 29123523]
- Wallet P, Benaoudia S, Mosnier A, Lagrange B, Martin A, Lindgren H, Golovliov I, Michal F, Basso P, Djebali S, et al. (2017). IFN- γ extends the immune functions of Guanylate Binding Proteins to inflammasome-independent antibacterial activities during *Francisella novicida* infection. *PLoS Pathog.* 13, e1006630.

- Wannamaker W, Davies R, Namchuk M, Pollard J, Ford P, Ku G, Decker C, Charifson P, Weber P, Germann UA, et al. (2007). (S)-1-((S)-2-[[1-(4-amino-3-chloro-phenyl)-methanoyl]-amino]-3,3-dimethyl-butanoyl)-pyrrolidine-2-carboxylic acid ((2R,3S)-2-ethoxy-5-oxo-tetrahydro-furan-3-yl)-amide (VX-765), an orally available selective interleukin (IL)-converting enzyme/caspase-1 inhibitor, exhibits potent anti-inflammatory activities by inhibiting the release of IL-1beta and IL-18. *J. Pharmacol. Exp. Ther.* 321, 509–516. [PubMed: 17289835]
- Weiss G. (2015). Anemia of Chronic Disorders: New Diagnostic Tools and New Treatment Strategies. *Semin. Hematol.* 52, 313–320. [PubMed: 26404443]
- Weissman IL (2000). Translating stem and progenitor cell biology to the clinic: barriers and opportunities. *Science* 287, 1442–1446. [PubMed: 10688785]
- Westerfield M. (2000). *The Zebrafish Book A Guide for the Laboratory Use of Zebrafish Danio* (Brachydanio rerio)* (Eugene, OR: University of Oregon Press).
- White RM, Sessa A, Burke C, Bowman T, LeBlanc J, Ceol C, Bourque C, Dovey M, Goessling W, Burns CE, and Zon LI (2008). Transparent adult zebrafish as a tool for in vivo transplantation analysis. *Cell Stem Cell* 2, 183–189. [PubMed: 18371439]
- Whyatt DJ, Karis A, Harkes IC, Verkerk A, Gillemans N, Elefanty AG, Vairo G, Ploemacher R, Grosveld F, and Philipsen S. (1997). The level of the tissue-specific factor GATA-1 affects the cell-cycle machinery. *Genes Funct.* 1, 11–24. [PubMed: 9680325]
- Whyatt D, Lindeboom F, Karis A, Ferreira R, Milot E, Hendriks R, de Bruijn M, Langeveld A, Gribnau J, Grosveld F, and Philipsen S. (2000). An intrinsic but cell-nonautonomous defect in GATA-1-overexpressing mouse erythroid cells. *Nature* 406, 519–524. [PubMed: 10952313]
- Wu WC, Sun HW, Chen HT, Liang J, Yu XJ, Wu C, Wang Z, and Zheng L. (2014). Circulating hematopoietic stem and progenitor cells are myeloid-biased in cancer patients. *Proc. Natl. Acad. Sci. USA* 111, 4221–4226. [PubMed: 24591638]
- Yang L, Wang L, Kalfa TA, Cancelas JA, Shang X, Pushkaran S, Mo J, Williams DA, and Zheng Y. (2007). Cdc42 critically regulates the balance between myelopoiesis and erythropoiesis. *Blood* 110, 3853–3861. [PubMed: 17702896]
- Zwack EE, Feeley EM, Burton AR, Hu B, Yamamoto M, Kanneganti TD, Bliska JB, Coers J, and Brodsky IE (2017). Guanylate Binding Proteins Regulate Inflammasome Activation in Response to Hyperinjected Yersinia Translocon Components. *Infect. Immun.* 85, e00778–16.

Highlights

- The inflammasome regulates the erythroid-myeloid decision in HSC
- Caspase-1 inhibition rapidly upregulates GATA1 protein in HSC
- Caspase-1 regulates terminal erythroid differentiation
- Caspase-1 inhibition rescues neutrophilic inflammation and anemia

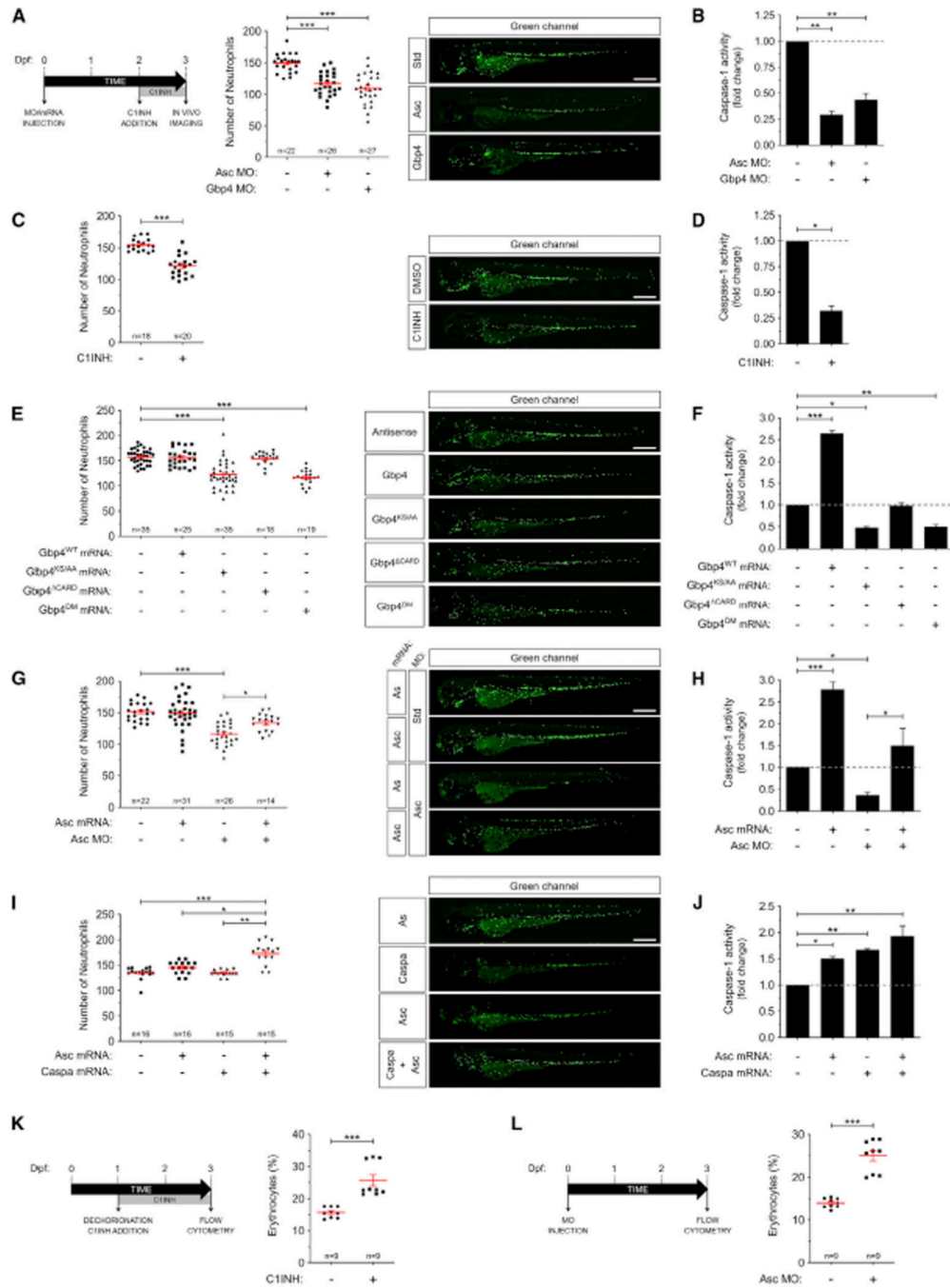


Figure 1. Inflammation Inhibition Results in Decreased Neutrophil but Increased Erythrocyte Numbers in Zebrafish

Tg(mpx:eGFP) (A-J) and *Tg(lcr:eGFP)* (L) zebrafish one-cell embryos were injected with standard control (Std), Asc, or Gbp4 MOs (A, B, G, H, L), and/or with antisense (As), Gbp4^{WT}, Gbp4^{KS/AA}, Gbp4^{CARD}, Gbp4^{DM}, Asc, or Caspa mRNAs (E-H). Alternatively, *Tg(mpx:eGFP)* (C, D, I, J) and *Tg(lcr:eGFP)* (K) embryos left uninjected were manually dechorionated at 24 or 48 hpf and treated by immersion with DMSO or the irreversible caspase-1 inhibitor Ac-YVAD-CMK (C1INH). Each dot represents the number of neutrophils (A, C, E, G, I) from a single larva or the percentage of erythrocytes from each

pool of 50 larvae (K, L), while the mean \pm SEM for each group is also shown. The sample size (n) is indicated for each treatment. Representative images of green channels of whole larvae for the different treatments are also shown. Scale bars, 500 μ m. Caspase-1 activity in whole larvae was determined for each treatment at 72 hpf (one representative caspase-1 activity assay out of the three carried out is shown) (B, D, F, H, J). * $p < 0.05$; ** $p < 0.01$; *** $p < 0.001$ according to ANOVA followed by Tukey multiple range test. See also Figures S1-S4.

Author Manuscript

Author Manuscript

Author Manuscript

Author Manuscript

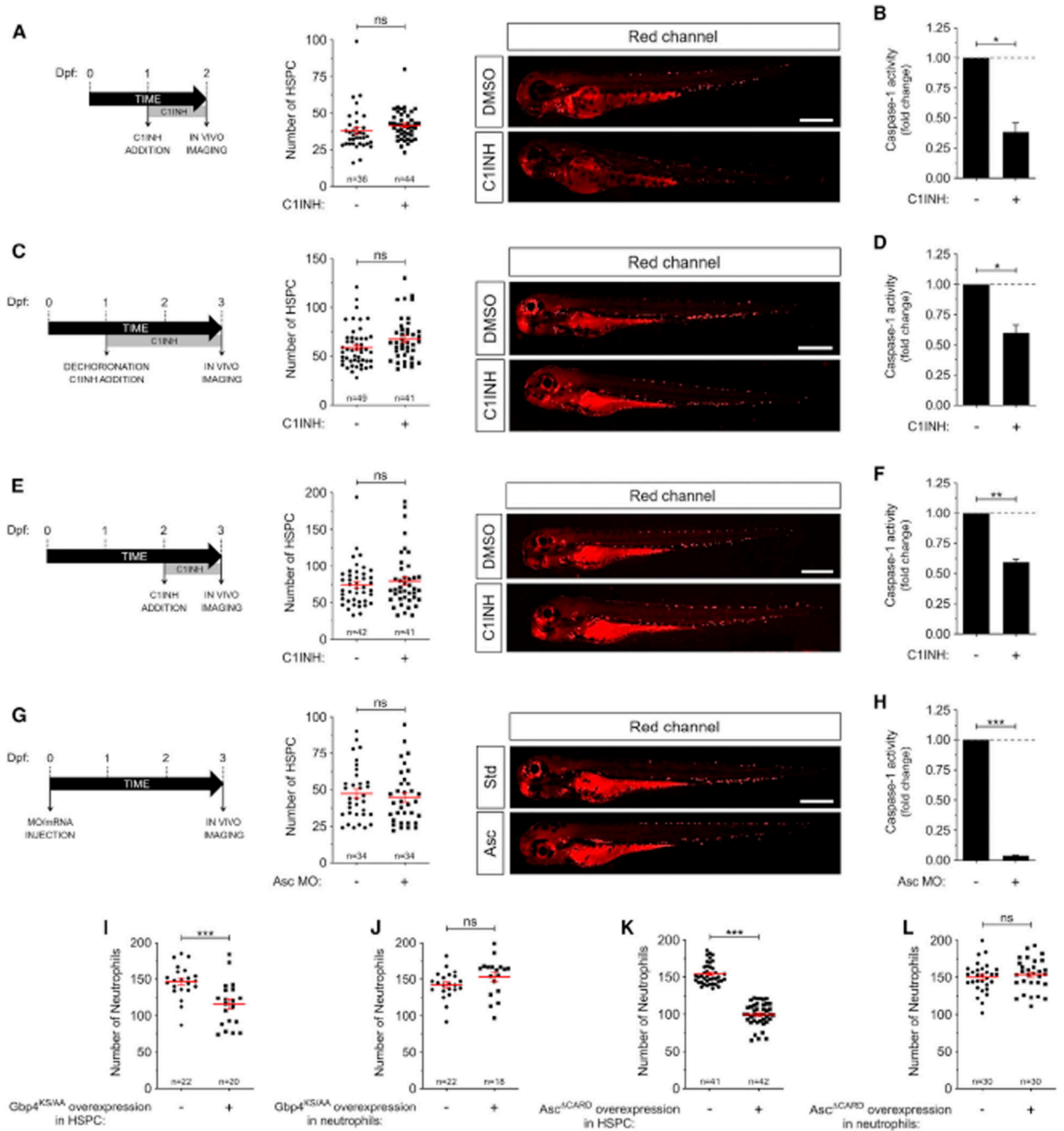


Figure 2. The Inflammasome Is Intrinsically Required for HSPC Differentiation but Is Dispensable for Their Emergence in Zebrafish
 (A-H) *Tg(runx1:GAL4; UAS:nfsb-mCherry)* zebrafish embryos were manually dechorionated at 24 or 48 hpf and treated by immersion with DMSO or the irreversible caspase-1 inhibitor Ac-YVAD-CMK (C1INH) for 24 or 48 h (A-F). Alternatively, *Tg(runx1:GAL4; UAS:nfsb-mCherry)* one-cell embryos were injected with standard control (Std) or Asc MOs (G-H). Each dot represents the number of HSPCs from a single larva, while the mean \pm SEM for each group is also shown. The sample size (n) is indicated for each treatment. Representative images of red channels of whole larvae for the different

treatments are also shown (A, C, E, G). Scale bars, 500 μm . Caspase-1 activity was determined for each treatment from 48 or 72 hpf larvae (one representative caspase-1 activity assay out of the three carried out is shown) (B, D, F, H).

(I-L) *Tg(runx1:gal4; UAS:Gbp4KS/AA)* (I), *Tg(mpx:gal4; UAS:Gbp4KS/AA)* (J), *Tg(runx1:gal4; UAS:Asc CARD)* (K), *Tg(mpx:gal4; UAS:Asc CARO)* (L) larvae were fixed at 72 hpf and stained with Sudan black for the detection of neutrophils. Each dot represents the number of neutrophils from a single larva, while the mean \pm SEM for each group is also shown. The sample size (n) is indicated for each treatment. ns, not significant; * $p < 0.05$; ** $p < 0.01$; *** $p < 0.001$ according to Student t test. See also Figure S4.

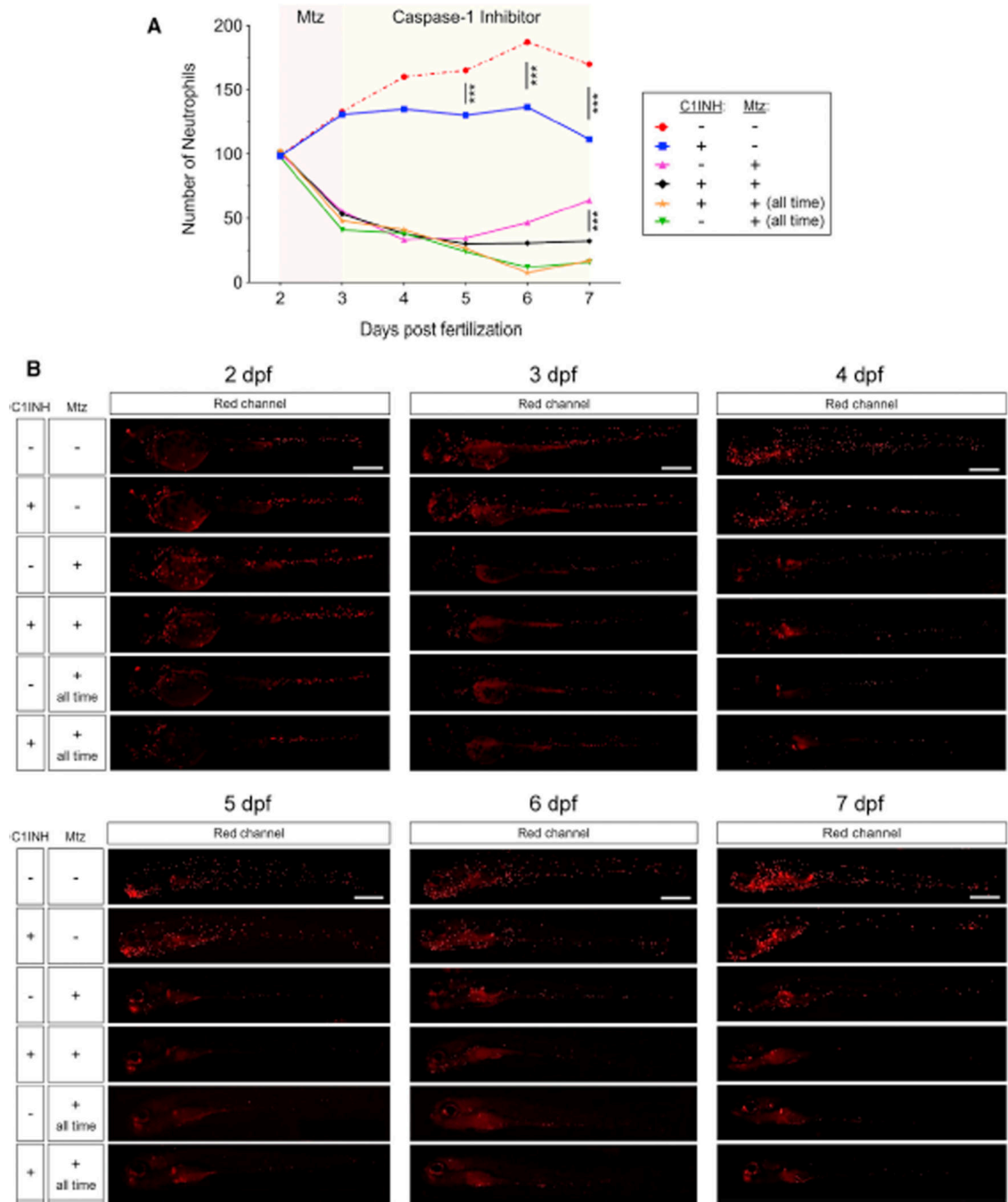


Figure 3. Inflammasome Activity Is Indispensable for Myelopoiesis in Zebrafish

Tg(mpx:GAL4; UAS:nfb-mCherry) zebrafish larvae were manually dechorionated at 48 hpf and treated by immersion with metronidazole (Mtz) for 24 h and then with DMSO or the irreversible caspase-1 inhibitor Ac-YVAD-CMK (C1INH) for the next 4 days. Control groups were treated for 5 days with Mtz (all time).

(A) Each dot represents the number of neutrophils from a single larva, while the mean \pm SEM for each group is also shown. Scale bars, 500 μ m. *** $p < 0.001$ according to ANOVA followed by Tukey multiple range test.

(B) Representative images of red channels of whole larvae for the different treatments and time points are also shown.

Author Manuscript

Author Manuscript

Author Manuscript

Author Manuscript

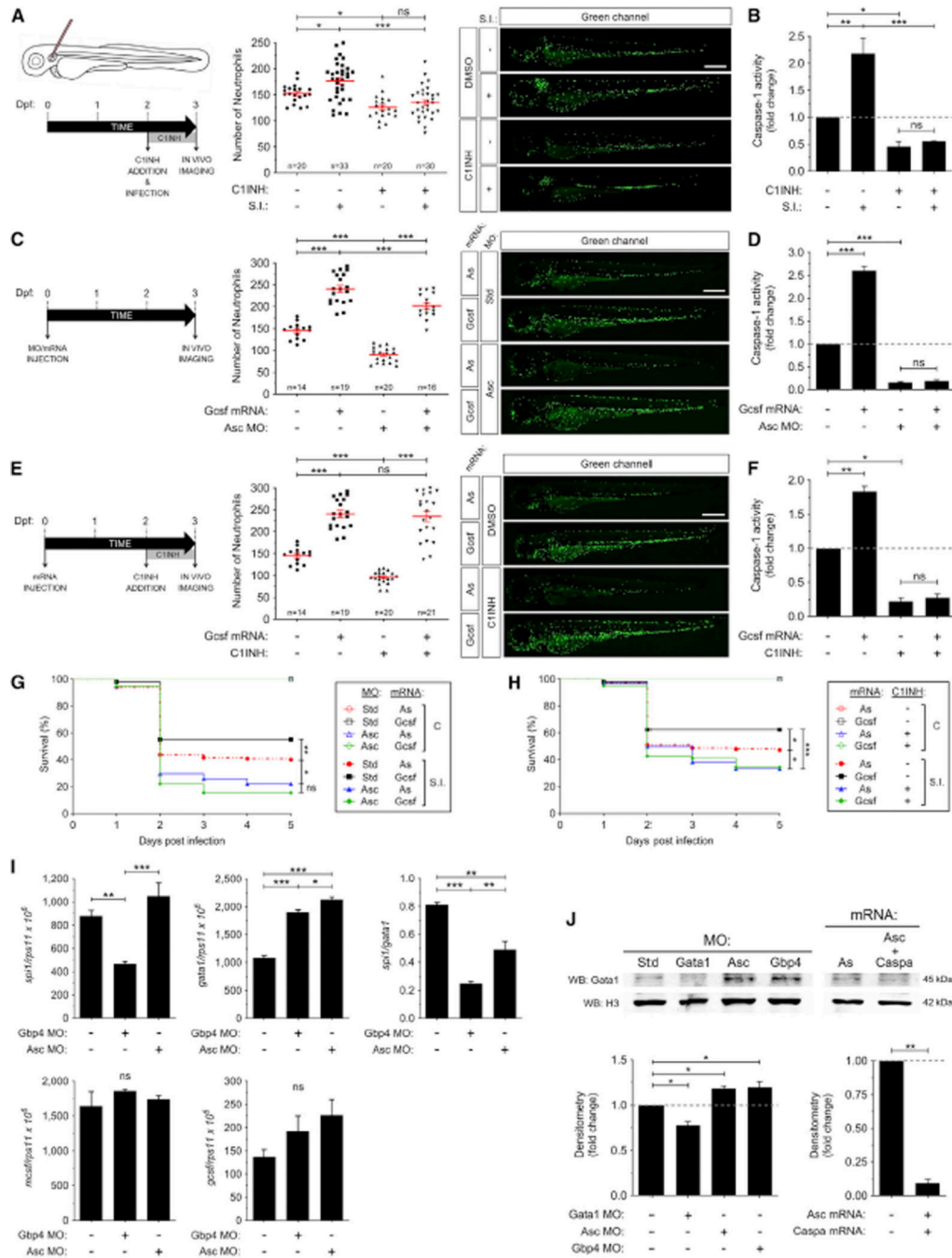


Figure 4. Infection Is Unable to Bypass the Inflammasome Requirement for Neutrophil Production in Zebrafish

(A-H) *Tg(mpx:eGFP)* zebrafish one-cell embryos were injected with standard control (Std), Gbp4, or Asc MOs in combination with antisense (As), Gcsfa, Asc, Caspa mRNAs (C, D, G, H-J) or left uninjected, manually dechorionated at 48 hpf and treated by immersion with DMSO or the irreversible caspase-1 inhibitor Ac-YVAD-CMK (C1INH) (A, B, E, F). Larvae were then infected at 48 hpf with *S. Typhimurium* (S.I.) in the otic vesicle (A, B) or the yolk sac (G, H) and the number of neutrophils was counted in the whole body at 24 hpi (A, B) or 72 hpf (C-F) and the survival was determined during 5 days after the infection (G, H).

H). Each dot represents the number of neutrophils from a single larva, while the mean \pm SEM for each group is also shown. The sample size (n) is indicated for each treatment. Note that the 4 non-infected group showed no mortality and the 4 lines are overlapping.

Representative images of green channels of whole larvae for the different treatments are shown (A-F). Scale bars, 500 μ m. Caspase-1 activity was determined in whole larvae for each treatment at 72 hpf (one representative caspase-1 activity assay out of the three carried out is shown) (B, D, F).

(I-J) The mRNA amounts of *spi1b*, *gata1a*, *mcsf*, and *gcsf* in larval tails were measured by RT-qPCR at 24 hpf (I), while the protein amounts of Gata1a and histone H3 were determined using western blot in larval tails at 24 hpf (J). A densitometry analysis was performed to check the differences between treatments. ns, not significant; *p < 0.05; **p < 0.01; ***p < 0.001 according to ANOVA followed by Tukey multiple range test (A-F, I, J) or log rank test with Bonferroni correction (G, H).

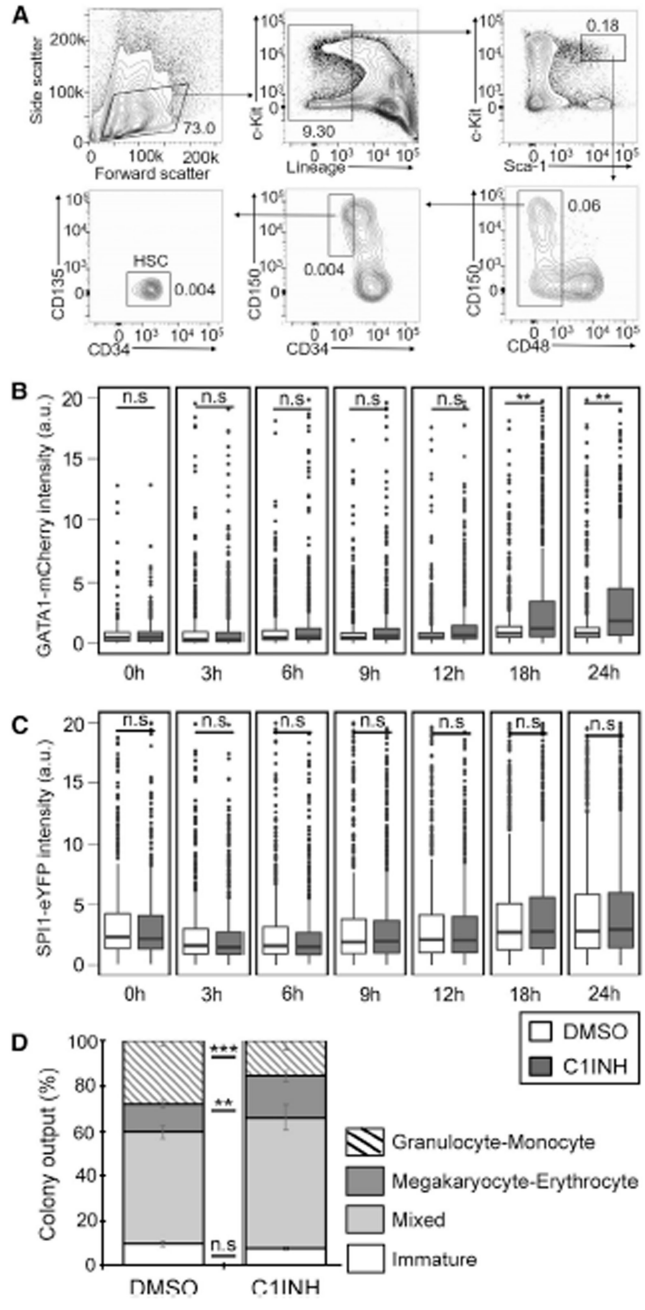


Figure 5. Inflammasome Inhibition Increases GATA1 Protein Amounts and Megakaryocyte-Erythrocyte Colony Output in Mouse HSCs

(A) Flow cytometry gating scheme used for isolation of mouse HSCs. HSCs are sorted as Lin⁻cKit⁺Sca1⁺CD48⁻CD34⁻CD135⁻CD150⁺. Numbers in the plots indicate % of lineage-depleted BM cells.

(B and C) Caspase1-inhibitor (C1INH) treatment increases GATA1 protein amounts (B) without affecting SPI1 protein amounts (C) in mouse HSCs. Data were acquired by time-lapse imaging of freshly-sorted HSCs (DMSO = 605, C1INH = 749 HSCs) from 12-week old SPI1-eYFP and GATA1-mCherry fluorescent protein fusion reporter mice in IMDM +

BIT + SCF + Epo + Tpo + IL3 + IL6 supplemented with or without 100 mM of the irreversible caspase-1 inhibitor Ac-YVAD-CMK (2 biological replicates).

(D) Caspase1-inhibitor treatment increased MegE colony output at the expense of GM colonies. HSCs from SPI1-eYFP and GATA1-mCherry reporter mice were single-cell sorted into 384 well plates in IMDM +BIT+SCF +Epo + Tpo + IL-3 + IL-6 supplemented with or without 100 μ M Ac-YVAD-CMK. At day 8, color conjugated CD41-APC and CD16/32-BV421 antibodies were added to the colonies and colonies were imaged and manually scored using morphology, SPI1-eYFP and CD16/32 signal to indicate GM colonies and GATA1-mCherry and CD41 signal to indicate MegE colonies. Data represent mean percentage of types of colonies formed from HSCs from 4 independent experiments (244 total colonies scored, error bars = SEM). ns, not significant; * $p < 0.05$; ** $p < 0.01$; *** $p < 0.001$ according to two tailed Student's t test (A, B) and Chi-square test (C).

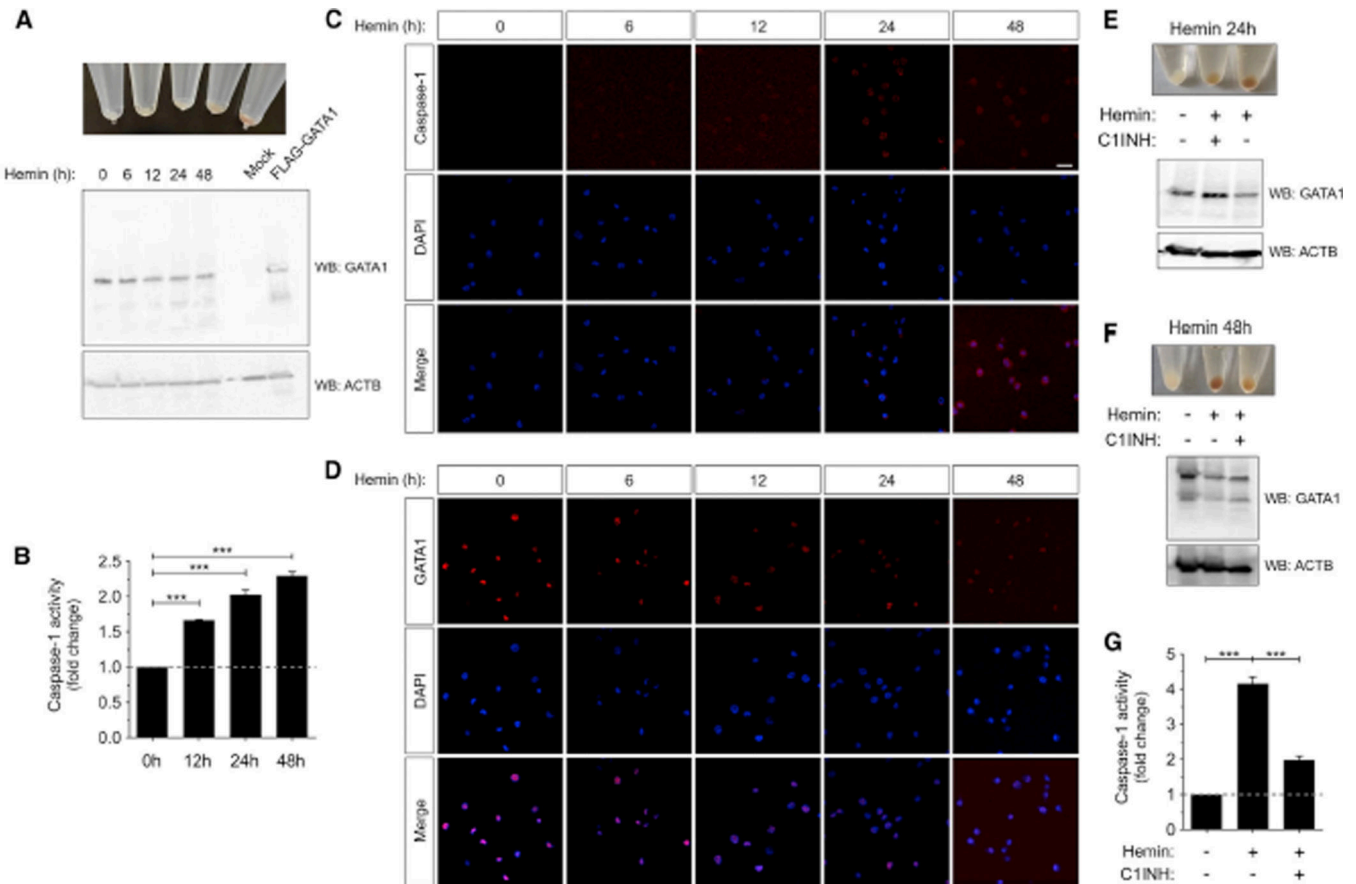


Figure 6. Pharmacological Inhibition of Caspase-1 Impairs Erythroid Differentiation of K562 Cells

K562 cells were incubated with 50 μ M hemin for the indicated times in the presence or absence of the irreversible caspase-1 inhibitor Ac-YVAD-CMK (C1INH, 100 μ M) and the cell pellets imaged (A, E, F), lysed and resolved by SDS-PAGE and immunoblotted with anti-GATA1 and anti-ACTB antibodies (A, E, F), processed for the quantification of caspase-1 activity using the fluorogenic substrate Z-YVAD-AFC (B, G) and for immunofluorescence using anti-CASP1 (C) and anti-GATA1 (D) antibodies. Cell extracts from HEK293T transfected with GATA1-FLAG and empty FLAG were included as mobility controls in (A). Nuclei were stained with DAPI. One representative caspase-1 activity (B, G), western blot (A, E, F) and hemoglobin accumulation (A, E, F) assay out of the three carried out is shown, while one representative immunofluorescence staining (C, D) assay out of the two carried out is shown. Scale bars, 5 μ m. *** p < 0.001 according to ANOVA followed by Tukey multiple range test. See also Figures S5–S7.

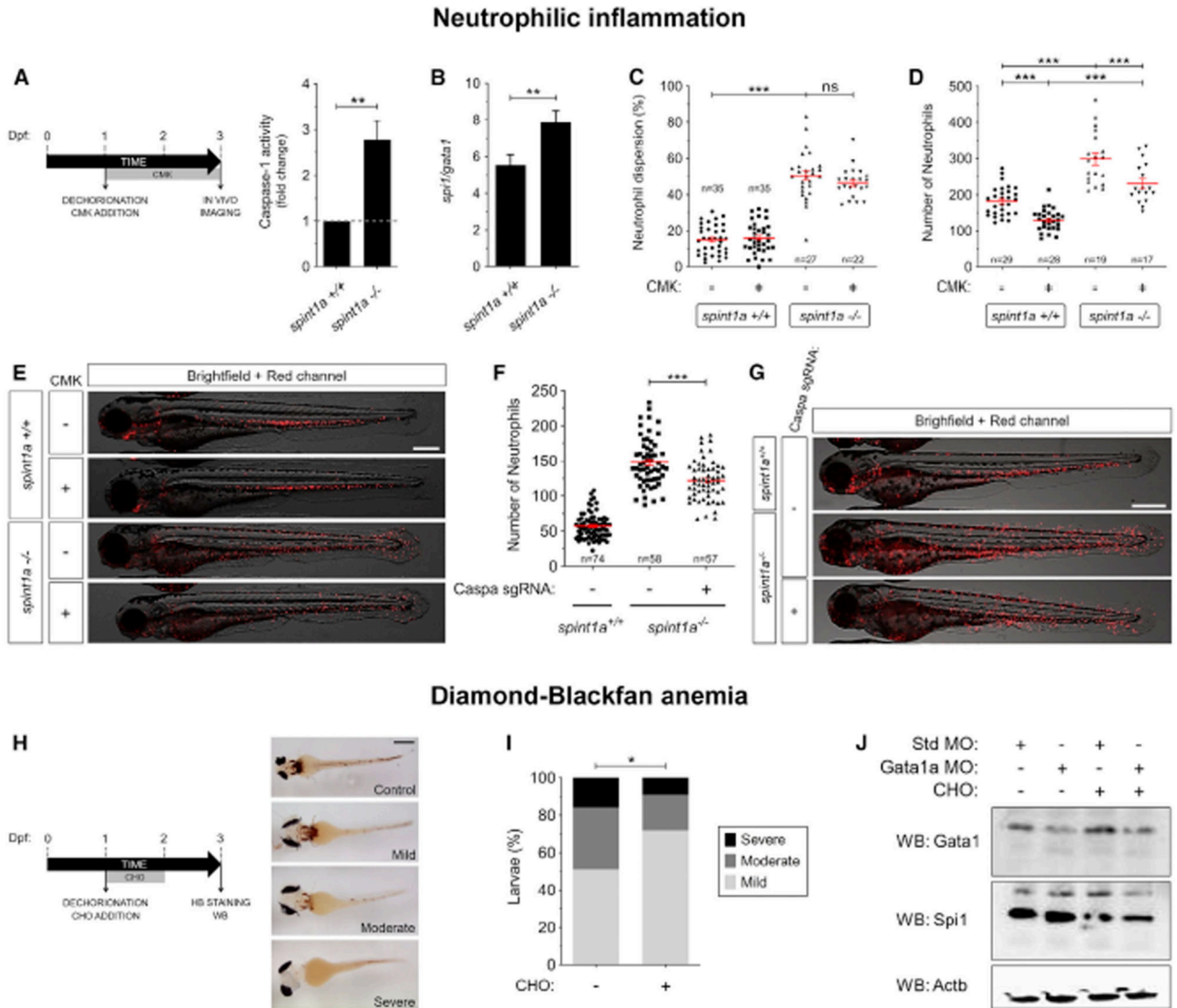


Figure 7. Pharmacological Inhibition of Caspase-1 Rescues Zebrafish Models of Neutrophilic Inflammation and Anemia

(A-G) Wild-type and *spint1a* mutant larvae were manually dechorionated and treated from 1–3 dpf with the irreversible caspase-1 inhibitor Ac-YVAD-CMK (CMK, 100 μ M) (A-E) or one-cell embryos injected with control (std) or *caspa* sgRNA and recombinant Cas9 (F, G). Caspase-1 activity (A), the *spi1b/gata1a* transcript expression ratio (B), neutrophil dispersion (C), and the number of neutrophils (D-G) were then determined. Each dot represents the number of neutrophils from a single larva, while the mean \pm SEM for each group is also shown. The sample size (n) is indicated for each treatment. Representative overlay images of green and bright field channels of whole larvae for the different treatments are shown (E, G). Scale bar, 500 μ m.

(H-J) Zebrafish one-cell embryos were injected with standard control (Std) or Gata1a MOs, manually dechorionated at 24 hpf and treated by immersion with DMSO or the reversible caspase-1 inhibitor Ac-YVAD-CHO (CHO) for 24–48 hpf. The inhibitor was then washed

off and the larvae incubated until 72 hpf. Representative pictures of Gata1a-deficient larvae with mild, moderate and severe anemia (H), quantification of the phenotype of larval treated with DMSO or Ac- YVAD-CHO (I) and immunoblot of larval extracts with anti-Gata1a, anti-Spi1b and anti-Actb antibodies (J). One representative caspase-1 activity (A) and western blot (J) assay out of the three and two, respectively, carried out is shown. ns, not significant; * $p < 0.05$; ** $p < 0.01$; *** $p < 0.001$ according to Student t test (A, B), ANOVA followed by Tukey multiple range test (C, D, F) and Fisher's exact test (I).

Author Manuscript

Author Manuscript

Author Manuscript

Author Manuscript

KEY RESOURCES TABLE

REAGENT or RESOURCE	SOURCE	IDENTIFIER
Antibodies		
Rabbit polyclonal to human GATA1	Santa Cruz Biotechnology	Cat#sc1234, RRID:AB_2263157
Rabbit mAb to human GATA1	Cell Signaling	Cat#3535, RRID:AB_2108288
Rabbit polyclonal to CASP1	Santa Cruz Biotechnology	Cat#sc56036, RRID:AB_781816
Rabbit polyclonal to zebrafish Gata1 a	GeneTex	Cat#GTX128333
Rabbit polyclonal to zebrafish Spi1 b	GeneTex	Cat#GTX128266
Rabbit polyclonal to histone H3	Abcam	Cat#ab1791, RRID:AB_302613
Monoclonal ANTI-FLAG® M2-Peroxidase (HRP) antibody produced in mouse	Sigma-Aldrich	Cat#A8592, RRID:AB_439702
Streptavidin-BV711	BD Biosciences	Cat#563262
anti-Sca1 conjugated with BV510	Biolegend	Cat#108129, RRID:AB_2561593
anti-cKIT conjugated with BV421	Biolegend	Cat#105828, RRID:AB_11204256
anti-CD135 conjugated with PerCPeFL710	Thermo Fisher Scientific	Cat#46-1351-82, RRID:AB_10733393
anti-CD34 conjugated with eFL660	Thermo Fisher Scientific	Cat#50-0341-82, RRID:AB_10596826
anti-CD48 conjugated with APCeFL780	Thermo Fisher Scientific	Cat#47-0481-82, RRID:AB_2573962
anti-CD150 conjugated with BV650	Biolegend	Cat#115932, RRID:AB_2715765
anti-B220-biotin	Thermo Fisher Scientific	Cat#13-0452-86, RRID:AB_466451
anti-CD19-biotin	Thermo Fisher Scientific	Cat#13-0191-86, RRID:AB_466386
antiCd3e-biotin	Thermo Fisher Scientific	Cat#13-0031-85, RRID:AB_466320
anti-CD11b-biotin	Thermo Fisher Scientific	Cat#13-0112-85, RRID:AB_466360
anti-Gr1-biotin	Thermo Fisher Scientific	Cat#13-5931-85, RRID:AB_466801
anti-Ter119-biotin	Thermo Fisher Scientific	Cat#13-5921-85, RRID:AB_466798
anti-CD41-APC	Thermo Fisher Scientific	Cat#17-0411-82, RRID:AB_1603237
anti-CD16/32-BV421	Biolegend	Cat#101332, RRID:AB_2650889
Bacterial and Virus Strains		
<i>Salmonella enterica</i> serovar Typhimurium, strain 12023 (wild type)	Prof. David Holden	
Chemicals, Peptides, and Recombinant Proteins		
EnGen® Cas9 NLS from <i>Streptococcus pyogenes</i>	New England Biolabs	Cat#M0646
Alt-R® CRISPR-Cas9 tracrRNA	Integrated DNA Technologies	Cat#1072532
Alt-R® CRISPR-Cas9 Negative Control crRNA	Integrated DNA Technologies	Cat#1072544
Ac-YVAD-CMK	Peptanova	Cat#3180-v
Ac-YVAD-CHO	Peptanova	Cat#3165-v
Ac-LEVD-CHO	Peptanova	Cat#864-42-v
Metronidazole	Sigma Aldrich	Cat#M1547
Sudan black	Sigma-Aldrich	Cat#380B-1KT
Z-YVAD-AFC	Merck	Cat#688225
ANTIFLAG® M2	Sigma-Aldrich	Cat#A2220

REAGENT or RESOURCE	SOURCE	IDENTIFIER
Recombinant caspase-1	GeneTex	Cat#GTX65025
4–15% SDS-PAGE	BioRad	Cat#456-1084
DNase I, amplification grade	ThermoFisher Scientific	Cat#18068015
SuperScript III RNase H ⁻ Reverse Transcriptase	ThermoFisher Scientific	Cat#18080085
Power SYBR Green Master Mix	ThermoFisher Scientific	Cat#4368708
Liberase TM research Grade	Sigma-Aldrich	Cat#05401119001
Protease inhibitor cocktail	Sigma-Aldrich	Cat#P8340
Hemin	Sigma-Aldrich	Cat#16009-13-5
ACK lysing buffer	Lonza	Cat#10-548E
RPMI-1640	Sigma-Aldrich	Cat#R0883
FCS	Cultek	Cat#91S181 D-050
Penicillin/Streptomycin	Sigma-Aldrich	Cat#P4333
Glutamine	Sigma-Aldrich	Cat#G7513
IMDM	ThermoFisher Scientific	Cat# 21056023
BIT	Stem Cell Technologies	Cat# 09500
IL3	Peprotech	Cat#213–13
IL6	Peprotech	Cat#216–16
SCF	Peprotech	Cat#250–03
EPO	Peprotech	Cat#100–65
TPO	Peprotech	Cat#315–14
Experimental Models: Cell Lines		
K562	ATCC	Cat#CCL243
Experimental Models: Organisms/Strains		
Zebrafish casper line (<i>roy^{a9/a9}, nacre^{w2/w2}</i>)	Prof. LI Zon	
<i>Tg(mpx:eGFP)^{j114}</i>	Prof. SA Renshaw	
<i>T9(mpe91:eGFP)^{el22}</i>	Prof. G Lieschke	
<i>T9(mpeg1:GAL4)⁹¹²⁵</i>	Prof. G Lieschke	
<i>Tg(lyz:dsRED)^{yz50}</i>	Prof. P Crosier	
<i>T9(mpx:Gal4.VP16)^{j222}</i>	Prof. SA Renshaw	
<i>T9(lcr:eGFP)^{z3325}</i>	Prof. LI Zon	
<i>T9(runx1:GAL4)^{wt6}</i>	Prof. LI Zon	
<i>T9(UAS:nfsB-mCherry)^{c264}</i>	Prof. M. Halpern	
<i>T9(spint1a)^{hi2217}</i>	Prof. M. Hammerschmidt	
SPI1-eYFP/GATA1-mCherry1 reporter mice (C57BL/6J background)	Prof. Timm Schroeder	
Recombinant DNA		
Tol2kit	Dr. K. Kwan	http://tol2kit.genetics.utah.edu/index.php/Main_Page